



Geologic Map and Database of the Roseburg 30 x 60' Quadrangle, Douglas and Coos Counties, Oregon

by Ray E. Wells¹, A.S. Jayko, A.R. Niem, G. Black, T. Wiley, E. Baldwin,
K.M. Molenaar, K.L. Wheeler, C.B. DuRoss, and R.W. Givler

Paleontological database by

D. Bukry, W. Elder, D. McKeel, L. Marincovich, W. Niem, and R.W. Givler

Prepared in cooperation with the Oregon Department of Geology and Mineral Industries

Open-File Report 00-376

2000

This report is preliminary and has not been reviewed for conformity with U.S. Geological Survey editorial standards or with the North American Stratigraphic Code. Any use of trade, firm, or product names is for descriptive purposes only and does not imply endorsement by the U.S. Government.

**U.S. DEPARTMENT OF THE INTERIOR
U.S. GEOLOGICAL SURVEY**

¹Menlo Park, California

INTRODUCTION

The Roseburg 30'x 60' Quadrangle covers the southeastern margin of the Oregon Coast Range and its tectonic boundary with Mesozoic terranes of the Klamath Mountains (Figures 1 and 2, also on map sheet). The geologic framework of the Roseburg area was established by the pioneering work of Diller (1898), Wells and Peck, (1961) and Ewart Baldwin (1974) and his students (Figure 3, also on map sheet). Baldwin and his students focussed on the history of the Eocene Tyee basin, where the sediments lap across the tectonic boundary with the Mesozoic terranes and record the accretion of the Coast Range basement to the continent. Others have examined the sedimentary fill of the Tyee basin in detail, recognizing the deep marine turbidite facies of the Tyee Formation (Snively and others, 1964) and proposing several models for the Eocene evolution of the forearc basin (Heller and Ryberg, 1983; Chan and Dott, 1983; Heller and Dickinson, 1985; Molenaar, 1985; see Ryu and others, 1992 for a comprehensive summary). Along the eastern margin of the quadrangle, both the Tyee basin and the Klamath terranes are overlain by Eocene volcanic rocks of the Western Cascade arc (Walker and MacLeod, 1991).

The thick Eocene sedimentary sequence of the Tyee basin has significant oil and gas potential (Armentrout and Suek, 1985; Gautier and others, 1993; Ryu and others, 1996). Although 13 deep test wells have been drilled in the Roseburg quadrangle (Figure 2 and Table 1, also on map sheet), exploration to date has been hampered by an incomplete understanding of the basin's tectonic setting and evolution. In response, the Oregon Department of Geology and Mineral Industries (DOGAMI) initiated a five year assessment of the oil and gas potential of the Tyee basin.

This map is a product of a cooperative effort by the U. S. Geological Survey, Oregon State University, and DOGAMI to systematically map the sedimentary facies and structure of the Tyee basin. New geologic mapping of twenty-eight 7.5' quadrangles is summarized on the map (Figure 3 also on map sheet), and the digital database contains geologic information suitable for both 1:100K and 1:24K scale analysis. DOGAMI has published a compilation and synthesis of previous mapping (Niem and Niem, 1990), a basin-wide sequence stratigraphic model and correlations (Ryu and others, 1992), and a report on the oil and gas potential (Ryu and others, 1996). Readers interested in the oil and gas potential of the Roseburg quadrangle should use the map in combination with Ryu and others (1996) to address specific stratigraphic units and structural plays.

Stratigraphic terminology for the Tyee basin adopts the type sections, formation names, and framework of Ryu and others (1992, 1996), which were developed concurrently with the mapping and are recognized throughout the basin. For detailed discussion of nomenclature, type sections, lithology, thickness and distribution, age, contact relationships, and depositional environment of stratigraphic units, the reader is referred to Ryu and others (1992). In this report we focus on the spatial, temporal, and structural relationships between units revealed by geologic mapping. Map unit ages (Figure 4, also on map sheet) are adjusted slightly from Ryu and others (1992, 1996) to fit new coccolith age determinations (D. Bukry, cited herein), paleomagnetic polarity data

(Simpson, 1977 and new data cited herein), and the time scale of Berggren and others (1995).

SUMMARY GEOLOGIC HISTORY

Geologic terranes in the Roseburg quadrangle record a history of continental margin sedimentation, magmatism, and terrane accretion from Jurassic to late Eocene time (Figure 2). In the southeastern part of the map area, two northeast-trending Mesozoic lithotectonic belts comprise the Western Klamath terranes. The oldest, the Jurassic Rogue continental arc complex and its sedimentary cover is thrust northwestward over melange, broken formation and semi-schists of the Cretaceous and Jurassic accretion complex represented by the Dothan Formation. The amalgamated Mesozoic terranes are in turn thrust northwestward over the Paleocene to lower Eocene Siletz River Volcanics, the oceanic basalt basement of the Oregon Coast Range. Overlapping the suture between the Siletz terrane and the Mesozoic rocks are sedimentary strata of the Eocene Tyee basin, which are also involved in the thrusting. Along the eastern margin of the quadrangle, Eocene volcanic units of the Western Cascade arc are deposited unconformably across the Tyee basin and the Mesozoic terranes.

Mesozoic terranes of the western Klamath Mountains

Jurassic continental arc complex and sedimentary cover

The Rogue volcanic arc consists of two parts; an intrusive sequence that includes predominantly hornblende gabbro, hornblende diorite, and diabase that are commonly slightly to strongly foliated, and extrusive rocks that include quartz keratophyre, keratophyre, plagioclase porphyry flows, pillows, hypabyssal dikes and flows, flow breccia, and minor tuffaceous sedimentary rock. These rocks are commonly tectonically brecciated and have undergone low to moderate greenschist facies metamorphism. The Rogue arc is part of the Western Klamath terrane, the Western Jurassic belt of Irwin, (1964), a remnant of an extensive volcanic arc and rifted arc complex (Harper and Wright, 1984) that lay along western North America during the Late Jurassic (Garcia, 1979, Garcia, 1982, Saleeby, et al., 1982, Ryberg, 1984). Similar rock associations to the southwest yield Late Jurassic and earliest Cretaceous radiometric ages (Dott, 1965, Saleeby, et al., 1982, Hotz, 1971, Harper and Wright, 1984). Imbricate thrust faulting and collapse of the arc during the Nevadan orogeny, which ranged in age between about 150 to 145 Ma in the Klamath region (Saleeby, et al., 1982, Harper and Wright, 1984) was syntectonic with, or was closely followed by deposition of the volcanolithic clastic rocks of the Myrtle Group. The Myrtle Group consists of Late Jurassic and Early to Middle Cretaceous turbidite and mass flow deposits considered to be either arc basin and/or post-orogenic flysh basins syntectonic with the waning phases of arc collapse (Imlay et al., 1959, Ryberg, 1984, Garcia, 1982, Roure and Blanchet, 1983).

Mesozoic Intrusive Complex

The intermediate and mafic igneous rocks of the Rogue arc and the pre-Nevadan sedimentary cover (Garcia, 1979) are intruded by siliceous and intermediate plutonic rocks principally of quartz diorite and granodiorite composition that are generally unfoliated or weakly foliated near the margins. Metamorphosed gabbroic to intermediate

country rock is locally preserved. The plutonic rocks are locally tectonized and consist of amphibolite, gneiss, banded gneiss and augen gneiss. Similar metamorphic rocks have yielded metamorphic ages of 165 to 150 Ma elsewhere in the westernmost Klamath terranes (Coleman, 1972, Hotz, 1971, Saleeby, et al., 1982, Coleman and Lanphere, 1991)

Cretaceous and Jurassic Accretion Complex

The Jurassic arc rocks and sedimentary cover are tectonic outliers (Figure 2) bounded to the northwest and southeast by melange, broken formation and semi-schist of the Dothan Formation or Sixes River terrane, which is part of the latest Jurassic and Cretaceous accretion complex (Ramp, 1972, Ryberg, 1984, Blake, et al., 1985). Plutonism that accompanied arc formation and tectonic collapse of the arc does not intrude the structurally underlying Dothan Formation, indicating major fault displacements since the Early Cretaceous. The Dothan Formation consists of low grade, sub-pumpellyite facies and pumpellyite bearing graywacke and semischistose graywacke, with scattered exotic blocks of blueschist, eclogite, greenstone, chert and limestone, including blocks of shallow water, Late Cretaceous Whitsett Limestone (Diller 1898). Semischistose and schistose rocks of the accretion complex have yielded metamorphic ages of around 125-140 Ma where they have been studied to the southwest (Coleman and Lanphere, 1971, Dott, 1965, Coleman, 1972). These rocks were unroofed and unconformably overlain by marine deposits by early Eocene time (Baldwin, 1974).

Cenozoic Terranes

Oregon Coast Range

Siletz River Volcanics

The submarine basaltic basement of the southern Oregon Coast Range is assigned to the Siletz River Volcanics, following the usage of Snively and others (1968), Molenaar (1985), Niem and Niem (1990), and Walker and MacLeod (1991). The thick sequence of Paleocene and early Eocene alkalic and tholeiitic pillow lava, submarine breccia, and capping subaerial flows are chemically and stratigraphically similar to the sequence exposed along the Siletz River in the type area (Table 4). Based on seismic and potential field studies, the basaltic basement, also known as the Siletz terrane, is geophysically continuous beneath the Coast Range, reaching a thickness of up to 35 km beneath the central Coast Range (Trehu and others, 1994). The Siletz River Volcanics and its correlative units in Washington and British Columbia (Crescent and Metchosin Formations; Snively and others, 1968) are thought to represent an oceanic plateau, island chain, or marginal basin that was accreted to the continent in the early Eocene (e.g., Simpson and Cox, 1977; Duncan, 1982; Wells and others, 1984; Clowes and others, 1987; Snively, 1987; Babcock and others, 1992).

In the Roseburg area, the Siletz River Volcanics are exposed in tightly folded anticlinal uplifts at Roseburg and at Turkey Hill. Lithologies are dominated by aphyric pillow basalt, with subordinate pillow breccia, lapilli tuff, aquagene laminated tuff, basaltic sandstone, and mudflow breccia. Lithic turbidite sandstone, mudstone, and conglomerate interbeds are common and appear to be derived from the Klamath Mountains, based on similarities with other Umpqua Group rocks. At Turkey Hill along the northern edge of

the map area, subaerial flows are exposed in the railroad cut east of I-5. The subaerial flows become more abundant to the north in the Drain area and presumably represent an emergent island volcanic center during Siletz River time (Hoover, 1963; Pyle, 1988, Ryu and others, 1992). Basaltic sandstone containing echinoderms, limpets and other rocky shoreline species are found above the subaerial flows at Turkey Hill and above vesicular pillowed flows about 5 km south of Nonpareil in the Roseburg anticlinorium (Figure 6, Table 2b and 2c). Along the axis of the Roseburg and Reston anticlinorium, sedimentary interbeds in the submarine basalt contain coccoliths assigned to the late Paleocene (locally CP 8?), whereas on the flanks of the uplift they are assigned to the early Eocene CP 10 zone where flows interfinger with Bushnell Rock Formation (Table 2a, Figure 5a and 5b; see also Bukry and Snively, 1988). The paleontologic ages (51.8 to 56 Ma, time scale of Berggren and others, 1995) are somewhat younger than five radiometric ages determined by Duncan (1982) from the Drain and Coquille River areas to the north and west of the quadrangle, which range in age from 62.1 ± 1.0 Ma to 59.2 ± 2.8 Ma. Paleomagnetic results from 19 flows in the Roseburg, Turkey Hill, and Coquille River area are all of reversed polarity (Table 3 and Figures 4 and 7), consistent with eruption during Chrons 23-24r in the Roseburg area (paleontologic range) and/or Chrons 25-27r in the Coquille-Drain area, if the radiometric ages are also correct.

The Siletz River Volcanics contains boulder, cobble, and pebble conglomerate interbeds of chert, limestone, greenstone, plutonic rocks, and metagraywacke derived from the Dothan Formation and Klamath terranes. Thick conglomerate interbeds are found in the oldest exposed basalt along I-5 and along Lookingglass Creek (late Paleocene) and in the upper kilometer of section where flows interfinger with the overlying conglomerate of the early Eocene Bushnell Rock Formation on the flanks of the Roseburg anticlinorium. Turbidite interbeds and pea gravels derived from Klamath source terranes are found throughout the 4 to 6 km thick volcanic section and are mapped as the Roseburg Member of the Siletz River Volcanics. The interbeds are lithologically similar to and correlative with the older part of the Umpqua Group (Bukry and Snively, 1988; Ryu and others, 1992) and are locally more abundant than pillow basalt.

Interbedded basalt and conglomerate derived from the Klamath Mountains requires a volcanic source close to the continental margin during eruption of the exposed 4 to 6 km-thick flow sequence. Late stage magmatism produced intrusions of diabase sills into the volcanic edifice and into the overlying Bushnell Rock Formation, commonly near thrust faults. Basaltic magmatism was apparently coeval with the early Eocene deformation of the basement and overlying Umpqua Group strata which resulted in juxtaposition against the Mesozoic accretionary complex.

Tyee Basin

Ryu and others (1992) recognized two superimposed basins with different trends and geologic histories in the southern Oregon Coast Range (Figure 2 on map sheet). The northeast-trending Paleocene to early Eocene Umpqua basin is filled with deformed turbidite sandstone and mudstone of the Umpqua Group. In the Roseburg map area, the basin is called the Sutherlin-Myrtle Point subbasin, which lies south of the Umpqua arch, an east-northeast-trending basement high of Siletz River Volcanics roughly coaxial with

the Turkey Hill-Millacoma anticline. Superimposed on the Umpqua basin is the north-south-trending Tyee forearc basin (Snively and others, 1964; Chan, 1982; Heller and Ryberg, 1983). The more gently deformed early and middle Eocene Tyee Formation is preserved in the broad synclinal low of the southern Oregon Coast Range, whereas the more structurally deformed Umpqua basin strata are exposed in broad antiformal highs on either side of the Coast Range syncline.

Composite thickness of the Umpqua-Tyee basin strata is about 20,000-ft (Ryu and others, 1992). The sedimentary sequence rests primarily on the Siletz terrane of the Oregon Coast Range and unconformably overlies Klamath Mountain terranes to the south. The mica-poor Umpqua Group is largely derived from accreted terranes of the Klamath Mountains and consists of conglomerate and sandstone of the Bushnell Rock Formation, the overlying turbidites of the Tenmile Formation, fluvial-deltaic strata of the White Tail Ridge Formation, and slope mudstone of the Camas Valley Formation. The Tyee forearc basin overlies the Umpqua Group on a regional unconformity. The abundantly micaceous strata are derived from older continental terranes to the east and consist of the deep marine and fluvial-deltaic Tyee Formation, the slope mudstone of the Elkton Formation and fluvial-deltaic sandstones of the Bateman and Spencer Formations.

In the map area, the Bushnell Rock Formation largely consists of clast supported boulder, cobble, and pebble conglomerate consisting of graywacke, chert, chert conglomerate, quartz, phyllite, metavolcanic, granitic, and basalt clasts mostly derived from the Mesozoic Klamath terranes. North of Dixonville, debris flows at the base of the formation contain blocks of Dothan up to 3 m in diameter in a basaltic mudflow matrix. Funglomerate, fan delta and deep marine turbidite channel facies occur in the conglomerates, which interfinger upsection with thick-bedded, fine grained sandstone facies of the Slater Creek Member. The formation is thickest along the southern margin of the Tyee basin, where it rests unconformably on the deformed Mesozoic terranes and Siletz River Volcanics. Although unconformable across tightly folded Siletz River Volcanics in the Reston anticline, deposition across the Wildlife Safari fault is syntectonic, and the conglomerate is involved in major thrusting along the Reston, Bonanza, and Wildlife Safari faults.

North and east of Roseburg, Bushnell Rock Formation interfingers with the pillow basalt of the Siletz River Volcanics and is intruded by diabase comagmatic with the pillow basalt. Mudstone interbeds at Roseburg contain coccoliths referable to the lower Eocene CP 10 zone, and at Glide, the conglomerate underlies Tenmile formation turbidites also referable to the CP 10 zone (Table 2a, Figure 5b). In the hills north and south of Glide, the Bushnell Rock Formation unconformably overlies the Siletz terrane along an oxidized, weathered contact and is fossiliferous, with abundant shallow water, rocky shoreline molluscan fauna within 100 m of the contact in several locations (Table 2b, Figure 6). The overlying Slater Creek member of the Bushnell Rock Formation is locally abundantly fossiliferous, with molluscan fauna indicating deposition under shallow water neritic conditions. The occurrence of shallow water facies and articulated molluscan fauna in the upper Bushnell Rock Formation, along with the lack of abrasion and significant transport at the above localities suggests the existence of a Klamath-derived

shoreline facies deposited across the Klamath Mountain-Coast Range suture during late Bushnell Rock time. This would have preceded deposition of the turbidites of the Tenmile Formation, which have long been interpreted as trench fill deposited on top of the accreted Siletz terrane (e.g. Heller and Ryberg, 1983).

The Tenmile Formation consists of classic turbidite basin deposits that overlie the Bushnell Rock Formation and fill the Sutherlin-Myrtle Point sub-basin. They consist of deep-marine inner, middle, and outer submarine fan turbidite sandstone sequences and basinal mudstones deposited in a marginal basin setting (Heller and Ryberg, 1983; Ryberg, 1984; Niem and Niem, 1990). Based on Mutti Ricci-Luchi (1972) and Walker and Mutti (1973) turbidite facies, we have subdivided the Formation into: 1) Tmcs, consisting of facies A and B, thick- to very thick-bedded, amalgamated sandstone and pebbly sandstone with mudstone partings interpreted as fan channel complexes; 2) Tmss, consisting of facies C and D, medium- to thick-bedded, rhythmic turbidite sandstone and mudstone interpreted as submarine fan depositional lobes; 3) Tmsm and Tmms, mostly medium to thin bedded facies C and D representing non-channelized fan deposition; and 4) Tmm, facies D and G, thin- to very thin-bedded turbidite sandstone, mudstone and thick mudstone, interpreted as basin plain deposits. These interpretations are generally consistent with those of Ryberg (1984), and indicate that the basin represents a complex turbidite fan sequence, with inner channel facies to the south and basin plain facies to the north at Turkey Hill. Deposition of the turbidites was also in part syntectonic (Perttu and Benson, 1980), based on current indicators which are locally parallel to fold axes in the Sutherlin sub-basin. Between Sutherlin and Umpqua, the upper Tenmile Formation (unit Tmsl) contains low angle turbidite channel sandstones, abundant slump folding, and soft sediment deformation consistent with deposition in a slope environment.

Coccoliths in the Tenmile Formation are assigned to the early Eocene CP 10 and 11 zones. In the map area, only one paleomagnetic site was sampled in what is now mapped as the Tenmile Formation, (Simpson, 1977 and Figure 7), and it is of normal polarity, consistent with the time scale of Berggren and others (1995). The CP 10-11 boundary (52.8 Ma) is found in the type area near Tenmile, in the lower part of the Glide section along the eastern edge of the quadrangle, in the Myrtle Point area just west of the quadrangle, and at the northern edge of the quadrangle in the lower most part of the basin plain sequence along I-5 just south of Turkey Hill (Figure 5; Table 2). The widespread occurrence of the CP 10-11 boundary allows us to correlate the turbidite sequences across the major thrust faults and assign them to the Tenmile Formation. Tenmile slope facies and overlying White Tail Ridge Formation rest on basin plain facies west of Metz Hill, indicating that the turbidite facies is older than the White Tail and Camas Valley part of the Umpqua Group in the Roseburg quadrangle, and it is not necessary to assign the basin plain facies to the Umpqua Group, undivided (cf Baldwin, 1974; Molenaar, 1985; Ryu and others, 1992).

An angular unconformity commonly separates the Tenmile Formation, which in many places is tightly folded, from the overlying, less deformed fluvial-deltaic strata of the White Tail Ridge Formation. However, the White Tail Ridge Formation is also involved in thrusting and folding along most of the major structures. As a result, the formation

forms three east-northeast-trending subbasins separated by structural highs along the Reston, Cooper Creek, and Oakland anticlines. West of the Umpqua River, the White Tail Ridge Formation was locally eroded or not deposited over these highs (see also Baldwin and Perttu, 1989; Black, 1990; Black and Priest, 1993). To the east, the White Tail thins over the highs, but is continuously exposed beneath the western Cascade volcanic sequence. Although the clean sandstone of the White Tail Ridge Formation is a potential reservoir, it may be restricted to the flanks of the sub-Tyee structures that are targets for hydrocarbon exploration. Its extent beneath the western Cascade sequence is unknown.

The White Tail Ridge Formation consists of four members; the basal shallow-marine Berry Creek member, the nonmarine Remote member, the delta front sandstone of the Coquille River member, and the shallow-marine Rasler Creek tongue, which interfingers with the slope mudstone of the overlying Camas Valley Formation (Ryu and others, 1992). The unit is locally fossiliferous; localities are shown in Table 2 and Figure 6.

The Berry Creek member consists of mollusk-bearing, bioturbated and hummocky bedded fine- to medium- grained, pebbly lithic arkosic sandstone in thickening- and coarsening upward sequences. The stratigraphic sequence in the thickening-upward cycles (i.e., hummocky bedded to parallel laminated to cross ripple laminated to trough cross-bedded sandstone) indicate that the Berry Creek member was deposited in wave-dominated shoreline or deltaic environment (Ryu and others, 1992). The overlying Remote member consists of ridge-forming, fining-upward sequences of cross-bedded, coarse-grained pebbly lithic arkosic sandstone, gray-green overbank mudstone, thin coals, and nonmarine fluvial to distributary channel conglomerate derived from the Klamath Mountains (Ryu and others, 1992; Ryberg, 1984). The Coquille River consists of mollusk-bearing, bioturbated to hummocky bedded, fine- to medium- grained, quartzofeldspathic sandstone, commonly as fining and thinning-upward sequences of thick, arkosic sandstone beds overlain by oyster-bearing estuarine mudstone, sandstone, and subbituminous coals. The unit represents a wave-dominated delta front facies, as does the overlying Rasler Creek tongue, which pinches out to the north (Ryu and others, 1992). Molluscan fauna in the White Tail Ridge Formation are characteristic of neritic environments and are of early Eocene age (Table 2b).

The uppermost formation in the Umpqua Group, the Camas Valley Formation, consists of massive, concretionary, locally fossiliferous, foraminiferal dark gray mudstone that interfingers with and overlies the Coquille River member of the White Tail Ridge Formation. The unit is mappable over a wide area, from the base of the Cascade volcanics to the western edge of the quadrangle and as far north as the Turkey Hill anticline. Coccoliths from the formation are referable to the CP-11 zone, or early Eocene (Bukry and Snavely, 1988). Several paleomagnetic sites in the Camas Valley Formation are of normal polarity (Simpson, 1977), also consistent with the paleontologic ages and the Berggren and others (1995) geomagnetic timescale (Figure 4).

The Tyee Formation records a change from the Umpqua Group in provenance and style of deformation (Diller, 1898; Heller and Ryberg, 1983; Heller and others, 1985). The

Tyee Formation consists of three abundantly micaceous members recognizable over the entire western half of the map area; the turbidites of the Tyee Mountain Member, slope mudstone of the Hubbard Creek Member, and fluvial deltaic sandstone of the Baughman Member (Baldwin, 1974; Molenaar, 1985; Ryu and others, 1992). The Tyee Mountain Member consists of up to two kilometers of rhythmically bedded, thick-bedded to massive, fine-grained, micaceous, light gray lithic arkosic sandstone and thin mudstones characteristic of turbidite facies B, C, and D of Mutti and Ricci Lucchi (1972) and Walker and Mutti (1973). The Hubbard Creek Member is a widely mappable unit consisting of thin-bedded, laminated micaceous gray siltstone and local channelized turbidite sandstone up to 300 m thick, interpreted as continental slope deposits (Ryu and others, 1992). In the map area, only one paleomagnetic site was sampled in the Hubbard Creek member, (Simpson, 1977 and Figure 7), but it is of reversed polarity, consistent with the time scale of Berggren and others (1995). The Baughman Member is thick- to very thick-bedded, micaceous, cross-bedded, lithic arkosic sandstone consisting of deltaic and fluvial facies. Lower delta plain and delta front facies are more common in the center of the basin where it is overlain by the Elkton Formation. The fluvial facies is widespread in the Roseburg area. The deltaic facies consists of three to four thickening-upward cycles of medium- to coarse-grained, mollusk-bearing, hummocky bedded, micaceous sandstone interstratified with thin gray mudstone.

Overlying the Tyee Formation is the Elkton Formation, a slope-forming, moderately indurated, laminated, dark gray micaceous mudstone up to 500 m thick. Foraminifers indicate deposition at bathyal depths (Bird, 1967). This unit is conformably overlain by the Bateman Formation (Weatherby, 1991) and interfingers with the underlying Baughman Member of the Tyee Formation. Bukry and Snively (1988) refer coccoliths from the Elkton Formation to Subzone CP12b, or early middle Eocene. Several paleomagnetic sites in the Elkton member are of normal polarity (Simpson, 1977), also consistent with the paleontologic ages and the Berggren and others (1995) geomagnetic timescale.

The Bateman Formation consists of delta front, distributary mouth bar, and distributary channel facies. Ryu and others (1992) describe the delta front facies as “composed of coarsening- and thickening-upward cycles (30-60 m thick) of thin- to thick-bedded, micaceous feldspathic wacke interstratified with subordinate, burrowed, massive mudstone and bedded to massive (bioturbated) siltstone (Weatherby, 1991). Individual sandstone beds are lenticular, massive, or parallel laminated to hummocky bedded. Graded bedding and microripple-laminations occur locally. Basal sandstone contacts are sharp and planar, although some display scour-and-fill structures. Laminations are enhanced by concentrations of disseminated carbonaceous plant debris and mica flakes.

Micaceous arkoses of the Spencer Formation up to 300 m thick crop out beneath the Cascade arc sequence to within three km south of Glide, where they are apparently overthrust by Jurassic serpentinized peridotite and Rogue volcanic rocks. The Spencer Formation is composed of several hundred feet of fluvial to deltaic, medium- to thick-bedded sandstone containing several subbituminous coal beds and thicker, laminated carbonaceous (leaf-bearing) mudstone-siltstone interbeds. The sandstone is friable,

micaceous arkosic, cross-bedded, and fine-grained to very coarse-grained sandstone. Shallow- marine mollusks and carbonaceous leaves date the formation as late Eocene (Hoover, 1963; Sanborn, 1937) just to the north of the map area. It is probably equivalent to, or slightly younger than the Bateman Formation and the Coaledo Formation of the Coos Bay basin.

Western Cascade arc

The late Mesozoic and early Cenozoic arc and forearc rocks are unconformably overlain to the east by the Eocene and younger continental fluvial deposits and volcanic rocks of the Cascade arc (Peck, et al., 1964, Baldwin, 1974, Walker and MacLeod, 1991). In the northeastern part of the map area, the basal units overlie the Spencer Formation and consist of altered, greenish gray volcanic sandstone, conglomerate, and andesitic mudflow breccia interstratified with lesser amounts of andesite flows, silicic ash flow tuff, and silicic lava flows. Basalt and basaltic andesite become more common upsection at Brown Mountain along the eastern quadrangle boundary. This sequence has been correlated with the Eocene Fisher Formation to the north of the quadrangle (Walker and MacLeod, 1991). To the south where the volcanic sequence is deposited on Klamath basement, the lowermost sedimentary strata contain significant non-volcanic continental deposits derived from the underlying granitic terrane. Locally, fossiliferous shallow marine sandstone is present at the base of the volcanic sequence. We have correlated this unit with the Eocene Colestin Formation described further south (Peck and others, 1964). The overlying andesite flows, mudflow breccias, and basalt are laterally continuous with the Fisher Formation to the north. Overlying the Fisher Formation are multiple cooling units of a regionally extensive ash flow sheet, the Tuff of Bond Creek, named for exposures just off the southeast corner of the quadrangle and K-Ar dated at 34.9 Ma (Smith and others 1982; Walker and MacLeod, 1991). Western Cascade basalt sills and dikes (gabbro, diabase, and norite) intruded Western Cascade volcanic units and underlying Tyee basin strata in the Eocene and Oligocene. Thick basalt sills occur in the White Tail Ridge Formation at the Colliding Rivers State Park area near Glide. Thin basalt sills also intrude the Tenmile Formation along the Oakland anticline, and in the Siletz River Volcanics near the bottom of Mobil's Sutherlin well. At 10,070-75 ft and 10,550-80 ft, the sills give late Eocene K-Ar ages of 33.9 ± 3.4 Ma to 36.8 ± 3.6 Ma (courtesy of Mobil Oil Corp., Bill Seeley, Lee High, and Neal R. Goins, 1989, written communication; Niem and Niem, 1990). An andesitic sill (?) similar to map unit Tia at the Rock Creek Guard station just off the edge of the quadrangle gives a K-Ar age of 28.5 ± 0.8 Ma (N. MacLeod, written communication, 1992).

Structure

The Roseburg Quadrangle can be divided, from oldest to youngest, into four northeast-trending tectonic belts separated by major thrust faults (Figure 2): 1) the Jurassic Rogue volcanic arc and sedimentary cover; 2) the Jurassic and Early Cretaceous accretionary complex of the Dothan Formation; 3) the Roseburg anticlinorium composed of the Paleocene-Eocene Siletz River Volcanics basement of the Oregon Coast Range; and 4) the early Eocene Umpqua basin fold and thrust belt. In the early Eocene, the Mesozoic terranes were thrust northwestward over the Siletz terrane, the basement of the Oregon

Coast Range, creating the syntectonic Umpqua basin along the continental margin. Folding and thrusting propagated into the basement, creating the Roseburg anticlinorium in the Siletz River Volcanics, which were in turn thrust over the Umpqua basin strata to produce the northwest-verging Umpqua fold and thrust belt. The early and middle Eocene Tyee Formation and the middle and late Eocene western Cascade lavas were subsequently deposited unconformably over the deformed tectonic belts.

Western Klamath Terranes

The structural grain of the Mesozoic rocks is dominated by north 30° to 40° east-trending faults and lithologic belts. The major faults separating Mesozoic units represent upper- and middle-crustal brittle structures, including high-angle oblique-slip reverse faults and associated overturned folds, deeper-seated north-west verging brittle and ductile shear zones within the plutonic complex, and transtensive, low-angle normal faults and detachment faults (Jayko, 1996a,b; Jayko, 1997; Jayko and Gallagher, 1997). The Dothan and Klamath rocks are separated by the Dodson Butte fault, a major northeast trending transpressive zone of imbricate faults that emplaces the Rogue arc complex and associated rocks over the Dothan complex. The igneous complex is locally overturned and is penetratively deformed into strongly banded and foliated gneiss, augen gneiss and mylonitic rock along major northwest verging, low angle thrust faults (Jayko, 1996a,b; Jayko, 1997; Jayko and Gallagher, 1997).

The contact between rocks of the Jurassic Rogue arc complex and the underlying siliceous plutonic rocks is typically characterized by a broad zone of cataclastic deformation, and the hanging wall and foot-wall rocks are commonly strongly foliated. Mineral assemblages associated with this deformation are typically lower greenschist facies with abundant secondary epidote, albite and pumpellyite. These faults and breccias zones are not invaded by magmatic fluids suggesting they are not syntectonic with the plutonism but were subsequent, in contrast to the intrusive contact relationships inferred from earlier mapping (Jayko, 1996a,b; Jayko, 1997; Jayko and Gallagher, 1997). The structural pendants of Rogue arc are locally strongly hydrothermally altered. Leaching of the mafic phases is common, particularly adjacent to high-angle normal faults.

Metamorphism

Regional, contact, and hydrothermal metamorphic rocks are all present within the study area. Regional metamorphic rocks include low to moderate-grade greenschist facies rocks of the arc complex that are inferred to have formed during the Nevadan orogeny of Late Jurassic age. Metamorphic rocks that formed during this event; which represents imbrication of the Late Jurassic arc, include gneiss, banded gneiss, augen gneiss and mylonitic rocks that are inferred to have originated at middle crustal levels (Jayko, 1996a,b; Jayko, 1997; Jayko and Gallagher, 1997). These rocks are typically upper greenschist and lower amphibolite facies.

Retrograde assemblages with epidote-pumpellyite and lower greenschist facies assemblages are commonly associated with cataclastic fabrics particularly near the major fault contacts which bound the arc complex units. This post plutonic semi-brittle deformation may be post-Nevadan and Cretaceous in age. The cataclastic fabrics are

inferred to have formed during extension associated with uplift and unroofing of the plutonic rocks (Jayko, 1996a,b; Jayko, 1997; Jayko and Gallagher, 1997).

Low-grade schists and semi-schists of prehnite-pumpellyite facies are characteristic of the higher-grade accretion complex rocks of the Dothan Formation in this area (Jayko, 1996a,b; Jayko, 1997; Jayko and Gallagher, 1997). These rocks generally structurally underlie major thrust faults that have the Rogue arc complex in the hanging wall. Schists of the Dothan Formation are generally partially reconstituted meta-sedimentary rocks with a moderately developed pressure solution fabric and incipient development of chlorite, white mica, and pumpellyite. Detrital tourmaline, epidote, biotite, muscovite, hornblende and pyroxene are common constituents of these rocks, but are not indicative of the metamorphic grade (Jayko, 1996a,b; Jayko, 1997; Jayko and Gallagher, 1997).

Hornfelsic hornblende gabbro rocks are locally present near the margins of large quartz diorite and granodiorite plutons. Hydrothermal alteration is widespread near high-angle faults that cut the Rogue volcanic rocks.

Oregon Coast Range and Western Cascade Arc

During the early Eocene, the Mesozoic arc, basin, and accretion complex were folded, thrust faulted, and partly unroofed during northwestward thrusting over early Cenozoic rocks of the Oregon Coast Ranges (Ramp, 1972, Baldwin, 1974, Champ, 1969, Ryberg, 1984). In the Coast Range, northwest-vergent thrusting created the northeast-trending Umpqua fold and thrust belt prior to deposition of the Tyee Formation (Baldwin, 1974). Near the Wildlife Safari fault, the Siletz terrane basement of the Coast Range is exposed in the core of the Roseburg anticlinorium, which is a complex, northwest-verging uplift of folded and thrust faulted Siletz River Volcanics.

The Wildlife Safari fault represents the major suture in the early Eocene between the Late Jurassic-Early Cretaceous accretionary complex and the late Paleocene-Eocene Coast Range terranes. This suture is interpreted to represent what remains of an early Tertiary subduction zone (e.g. Heller and Ryberg, 1983). The fault has a scalloped map trace consistent with a thrust geometry, but we observed it at only one location at an abandoned quarry at the Wildlife Safari game park. There it juxtaposes Dothan Formation graywacke and blueschist against conglomeratic debris flow (Tbr) and pebbly laminated mudstone intruded by diabase of Siletz River affinity. The fault zone is 30 m wide and locally trends 300°, with north side-down motion on multiple fault strands dipping 60-70° to both north and south, and abundant slickensides plunging 70° toward 030°. In the Dothan Formation adjacent to the fault, exotic blocks of blueschist, chert, greenstone, diorite, and eclogite tend to be concentrated in a melange zone a few hundred meters wide.

Deposition of the Bushnell Rock Formation was syntectonic with movement on the Wildlife Safari fault. East of the type section at Bushnell Rock, the conglomerate is caught up in the fault zone, and at several localities between Lookingglass Creek and Dixonville, the conglomerate beneath the fault contains matrix supported conglomeratic

debris flow deposits containing large, angular blocks of graywacke and greenstone derived from the Dothan Formation in the upper plate.

Evidence of a late Mesozoic or early Cenozoic subduction complex is lacking along the Wildlife Safari fault in the Roseburg quadrangle. The only age from the Dothan melange along or near the fault contact is Early Cretaceous (Table 2a). The lower zeolite facies pillow basalt of the Siletz terrane and the relatively coherent, unmetamorphosed sedimentary units in lower plate have no penetrative fabric to compare with that seen along the southeastern margin of the older Dothan accretionary complex, where the rocks are phyllitic or semi-schistose. It seems unlikely that the exposed Siletz terrane has been subducted to any great depth along the Wildlife Safari fault (see Tectonic Models, below for further discussion). The Wildlife Safari fault however, continued to move during and following deposition of the White Tail Ridge Formation. East of Dixonville, the White Tail Ridge Formation is isoclinally folded beneath the Wildlife Safari and Dotson Butte thrust fault. In general, folding in the lower plate is coaxial with thrusting and suggests that lateral motion on the Wildlife Safari fault is less than the thrust motion. The imbricate package of broken formation and melange in the Dothan formation is also folded around axes that are roughly coaxial with those in the Siletz River Volcanics in the lower plate, indicating that both upper and lower plate and the intervening thrust have been deformed by continued folding.

In the Roseburg anticlinorium, which lies between the Wildlife Safari fault and the Reston-Bonanza fault, the Siletz River Volcanics are folded into open, northwest-vergent folds, commonly bound on the northwest by thrust faults (see cross section B-B'). Isoclinal folding is common near the thrusts, which generally strike N 25-60°E and dip 40-70° SE. Fault slip directions trend 285-315°, indicating northwest to slightly right-oblique directed thrusting. Large lateral motions across the thrusts are limited by a west-northwest channel of Bushnell Rock conglomerate, which is repeated six times along the North Umpqua River by a series of thrusts, with little lateral offset. The oldest Tertiary rocks in the Coast Range are exposed along the axis of the anticlinorium between Reston and east Roseburg, where late Paleocene coccoliths are found in mudstone interbeds in the pillow basalt (Table 2a, Figure 5a-b). Toward Reston, the basalt thins and interfingers with late Paleocene turbidites of the Roseburg Member, which are exposed beneath the basalt in the anticlinal core.

The northern boundary of the Roseburg anticlinorium is the Reston-Bonanza fault, where the Siletz River Volcanics and the Bushnell Rock Formation, locally intruded by altered diabase sills of Siletz affinity, are thrust northwestward over mid-fan turbidites of the Tenmile Formation. The fault is exposed at several localities. Along I-5 at Wilbur, three fault strands dipping 40-70° S crop out over 250 m and exhibit a complex history of thrusting and normal-dextral reactivation. Along the Sutherlin Creek BLM Road (NESW1/4 29, 25S R4W), the fault is relatively simple, putting basaltic tuff and mudflows over pebbly turbidites on a fault locally trending 023/44°E, with a slip direction of 285°. Northeast of the Sutherlin Creek Road locality, the fault cuts through white, argillically altered, sulfide and quartz-bearing, fractured turbidite sandstone that can be mapped northeastward, beyond the Bonanza and Nonpareil mercury mines, for

about 20 kilometers along the fault zone (see Wells and Waters, 1934). This alteration may be related to reactivation of the fault during early Cascade arc magmatism; the fault clearly offsets the Spencer Formation and the Eocene volcanics, which are also altered and folded into an anticline/syncline pair and are standing vertically along the fault zone. To the west, the older Tyee Formation is not offset by the fault, which continues westward beneath the Tyee to re-emerge in the Remote area.

To the north, the Cooper Creek thrust emplaces thick bedded mid fan turbidite sandstone over thin bedded sandstone, basin plain mudstone, and younger White Tail Ridge Formation. Although poorly exposed, the Cooper Creek structure appears to be an important element in controlling the distribution of the nearshore White Tail Ridge Formation and the subsequent deformation of the overlying Tyee Formation. En echelon anticlines trend WSW across the Tyee basin along the projection of the Cooper Creek thrust, through the Williams River area toward the Middle Creek fault zone on the west side of the Tyee basin. Although small synclinal troughs of White Tail Ridge Formation occur to the north of this structure, most of the White Tail lies to the south of the Cooper Creek thrust.

North of the Cooper Creek thrust, five basalt cored anticlines form a northeast-striking fold belt extending 30 km beyond the quadrangle boundary; including the Oakland, Heavens Gate, Turkey Hill-Dickenson Mountain, Drain, and Jack Creek anticlines. In the Oakland and Heavens Gate anticlines, the basalt is not exposed at the surface, but is inferred from aeromagnetic highs along the fold crest (U. S. Geological Survey, 1999), and it is encountered at a depth of 4300' in the Mobil Sutherlin #1 exploration well on the crest of the Oakland anticline (Table 1). At Turkey Hill, vesicular, red oxidized subaerial basalt over pillow basalt is exposed in the anticlinal axis, which appears to extend west-southwest into the Tyee basin as the Millacoma anticline. The composite Heavens Gate-Turkey Hill-Millacoma anticline coincides with the Umpqua arch, a partly constructional basement high of Siletz River Volcanics encountered in the B-1 and F-1 wells at 6900' and 4400' respectively, that separates the Sutherlin-Myrtle Point subbasin from the Smith River subbasin to the north (Ryu and others, 1992, 1996). The Umpqua arch may represent the northern limit of preservation of the White Tail Ridge Formation in synclinal troughs beneath the Tyee basin strata.

In the Tyee basin, an unconformity at the base of Tyee Formation truncates most of the major northeast-trending folds of Umpqua Group, but minor folding continued after Tyee time along the Turkey Hill-Millacoma and Williams River uplift. Later folding (Miocene?) of the Tyee along N-S and NW axes has refolded the older northeast fold trends, creating complex, but subtle dome and basin structures in the Tyee basin (Figure 2). The northwest-trending Burnt Ridge anticline appears to be following an old pre-Tyee high (Wiley and others, 1994; Black, 1990), whereas the Williams River uplift appears to be a domal structure formed by fold interference between the Cooper Creek trend and the later, more northerly fold trends. The Williams River high appears to divide and deflect the Coast Range Syncline around its flanks. Although the dips on the flanks of the domal structures are generally less than 10-15°, the domes may represent modest hydrocarbon targets, if suitable closure can be demonstrated and the distribution of the

White Tail Ridge Formation at depth can be determined. More detailed discussion of these and other potential hydrocarbon traps, keyed to our new geologic mapping, can be found in Ryu and others, 1996.

Tectonic models

The boundary fault between the Coast Range mafic basement and the pre-Tertiary terranes of North America is only exposed in two places; southern Vancouver Island and southwestern Oregon near Roseburg. Field relationships observed in the Roseburg area provide information that could help distinguish between the two competing tectonic models for the origin and emplacement of the oceanic basement of the Coast Range: 1) collision and accretion of a hot spot generated oceanic island chain or oceanic plateau during subduction (e.g., Simpson and Cox, 1977; Duncan, 1982; Heller and Ryberg, 1983; Wells and others, 1984); and 2) formation of the Siletz terrane during hotspot-related oblique rifting of the continental margin and subsequent accretion of the marginal basin (Wells and others, 1984; Clowes and others, 1987; Snively, 1987; Babcock and others, 1992).

In the collision model, the Eocene suture along the Wildlife Safari fault represents a paleosubduction zone clogged by accreted oceanic islands of the Siletz terrane and its associated trench turbidites. Heller and Ryberg (1983) have suggested that the Tyee basin fill records the transition from subduction to forearc basin following the collision of the seamount terrane and resulting westward step of the subduction zone. In the alternative model, the Siletz terrane represents a marginal rift basin created during a period of Kula-North American plate dextral shear and Yellowstone hotspot volcanism in the Eocene (Wells and others, 1984; Clowes and others, 1987; Snively, 1987; Babcock and others, 1992). Accretion would have followed migration of the Kula-Farallon triple junction northward and the subsequent change in plate motion to more normal Farallon subduction.

The collision model explains very well the origin of the oceanic basalt, its deformation, accretion to the continent, the syntectonic basin fill, and the relatively low heat flow in the basin inferred from vitranite reflectance (Ryu and others, 1996). On the other hand, the lack of a Late Cretaceous-early Tertiary accretionary complex and subduction-related metamorphism in the Tertiary lower plate of the Wildlife Safari fault is puzzling. Turbidites of the Tenmile Formation previously inferred to be trench fill are now known to overlie shallow water facies of the Slater Creek member of the Bushnell Rock Formation, which was deposited on both pre-Tertiary and Siletz terranes (see also Ryu and others, 1992). The intimate interbedding of Paleocene and early Eocene Roseburg Member turbidites and conglomerate with the Siletz River Volcanics requires the oldest part of the Siletz terrane to be formed in close proximity to the Klamath margin between 56 and 52 Ma, which is hard to reconcile with predicted rapid northeast plate motions offshore (Engelbreton and others, 1985). The Siletz River Volcanics also represent the beginning of a 30 million year history of extensional basaltic and alkalic magmatism in the Coast Range, not easily explained by accretion of an oceanic island or plateau.

Continental margin rifting explains the prolonged history of mafic extensional magmatism in the Oregon Coast Range and fits better with predicted Kula-Farallon-North America plate motion history in the early Tertiary. The conglomerate interbedded with the pillow basalt is easy to reconcile with a rift basin origin for the Siletz terrane, as is the lack of a well developed subduction complex along the terrane boundary fault. Not so easily explained is the occurrence of major thrusting during the initial stages of basin filling, which is more consistent with convergence. Mafic dike swarms of Siletz River affinity that could represent the initiation of rifting have not been recognized in the adjacent pre-Tertiary terranes. One might also expect higher Eocene heat flow than is observed, if the basin was rift related.

Given the difficulties with both models, the origin of the Coast Range basement may be a unique event resulting from complex interactions between the continental margin, oceanic plates that were reorganizing in the early Eocene, and possible hotspot volcanism. Although further discussion of Siletz terrane origins is beyond the scope of this investigation, it is worth considering the possibility that the old subduction zone is hidden beneath the Siletz terrane in the Roseburg quadrangle (Figure 8), similar to what is inferred for the northeastern Solomon Islands of the southwest Pacific (Kroenke, 1984). In the Solomon Islands, the Miocene collision of the Ontong Java Plateau with the Solomons arc has obducted part of the oceanic plateau onto the arc platform, overriding the subduction zone while the oceanic plate continued to subduct beneath the arc (eg. Cooper and others, 1986). The northeastern Solomon islands of Malaita and Santa Isabel represent the emergent part of the obducted plateau and comprise a fold and thrust belt cored with oceanic basalt, much like the Roseburg anticlinorium and the Umpqua fold belt. Turbidites are being deposited in the North Solomons trough created by downwarping of the obducted Ontong Java Plateau above the still sinking slab (Kroenke, 1989), analogous to the Tenmile Formation near Roseburg. In the Solomon Islands, the subduction complex is largely hidden beneath the obducted oceanic terrane. Deep geophysical investigations across the Coast Range boundary may help resolve the existence of a similar structure in the Roseburg area.

Although the origin of the Siletz terrane is debatable, there are important constraints on the geometry of accretion and the orientation of the early Eocene continental margin revealed by the new geologic mapping and existing paleomagnetic investigations in the Tyee basin. Paleomagnetic results from early Eocene through Miocene volcanic and sedimentary rocks from coastal Oregon indicate about 75° clockwise rotation of the Oregon Coast Range with respect to stable North America since the early Eocene (e.g., Simpson and Cox, 1977; England and Wells, 1991), a rotation that may still be occurring today (e.g., Wells and others, 1998). Additional paleomagnetic data presented here (Table 4, Figures 6 and 9) and summarized in Wells and others (1985), indicate $79^\circ \pm 13^\circ$ clockwise rotation of Siletz River basalt flows in the Roseburg area, consistent with results from the Siletz terrane in the rest of the Oregon Coast Range. The paleomagnetic data passes the fold test, and the flows are all of reversed polarity, which in the Berggren and others (1995) time scale is consistent with paleontologic and Ar/Ar ages.

The overlying, relatively undeformed Tyee Formation is rotated about 67° clockwise (Simpson and Cox, 1977), and its onlap onto the Klamath terranes indicate that the rotation largely post dates accretion of the Siletz terrane to the continent (e.g., Heller and Ryberg, 1983). This information can be used to reconstruct the orientation of the continental margin at the time of accretion. Given that the overlying Tyee is rotated 67°, rotation of the Siletz terrane prior to deformation against the pre-Tertiary margin must have been small. On the other hand, the Umpqua fold axes formed prior to deposition of the Tyee must have rotated at least 67° clockwise after their formation. The lack of post-folding structures in the Tyee needed to accommodate small block rotation indicates that the rotation must have occurred as a relatively large block. Because the Umpqua folds are parallel to the Wildlife Safari terrane boundary fault and the structural trends in the Western Klamath terrane, we assume the early Eocene fold trends (after subtracting the paleomagnetic rotation) indicate the orientation of the margin at the time of accretion. By the same logic, we reconstructed the early Eocene continental margin for the rest of Oregon and Washington by assuming that the margin was parallel to Eocene folds mapped in the Siletz River Volcanics and Crescent Formation elsewhere in the Coast Range (Figure 10). Fold axes based on over 1000 poles to bedding for the Siletz River Volcanics of Oregon and the correlative Crescent Formation of Washington (Wells and Coe, 1985; Wells, 1989, unpublished data), when corrected for tectonic rotation, provide a coherent picture of the paleo-continental margin trending about N 30° W in Oregon and about N 60° W in Washington. This margin is less embayed than in earlier reconstructions and provides some constraints on the distribution and eastward extent of continental margin sedimentary basins in the Pacific Northwest.

ACKNOWLEDGMENTS

This map is the product of a cooperative mapping project involving the U. S. Geological Survey, the Oregon Department of Geology and Mineral Industries, and Oregon State University. Able field assistance was provided by Mike Gallagher, Lars Cherichetti, Brett Smith, Cheryl Hummon, Tracey Felger, Mark Abolins, and Mike Sinor. Additional GIS compilation and analysis were provided by Rob Givler, Chris DuRoss, Johanna Fenton, Tracey Felger, and Mike Sinor. Discussions with David Bukry, William Seeley, Parke D. Snively III, and reviews by Parke D. Snively, Jr. are gratefully acknowledged. We thank the Weyerhaeuser Corporation, Sun Studs of Roseburg, Roseburg Lumber, T. Weasma of the Bureau of Land Management, M. Wilson of the Oregon Department of Transportation, and the people of Douglas and Coos County for their assistance.

REFERENCES

Almgren, A. A., Filewicz, M. V., Heitman, H. L., 1988, Early Tertiary foraminiferal and nannofossil zonation of California; an overview and recommendation, *in* Filewicz, M. V. and Squires, R. L., eds., *Paleogene stratigraphy, West Coast of North America: Society of Economic Paleontologists and Mineralogists Pacific Section, West Coast Paleogene Symposium*, v. 58, p. 83-105.

Armentrout, J. M. and Suek, D. H., 1985, Hydrocarbon exploration in western Oregon and Washington: American Association of Petroleum Geologists Bulletin, v. 69, no. 4, p. 627-643.

Babcock, R. S., Burmester, R. F., Engebretson, D. C., and Warnock, A., 1992, A rifted margin origin for the Crescent Basalts and related rocks in the northern Coast Range volcanic province, Washington and British Columbia: Journal of Geophysical Research, v. 97, p. 6799-6821.

Baldwin, E. M., 1961, Geologic map of the lower Umpqua River area, Oregon: U.S. Geological Survey Oil and Gas Investigations Map OM-204, scale 1:62,500.

Baldwin, E. M., 1974, Eocene stratigraphy of southwestern Oregon: Oregon Dept. of Geology and Mineral Industries Bulletin 83, 40 p.

Baldwin, E. M. and Beaulieu, J. D., 1973, Geology and mineral resources of Coos County, Oregon: Oregon Dept. of Geology and Mineral Industries Bulletin 80, p. 9-40.

Baldwin, E. M. and Perttu, R. K., 1989, Eocene unconformities in the Camas Valley quadrangle, Oregon: Oregon Geology, v. 51, no. 1, p. 3-8.

Berggren, W.A., Kent, D.V., Swisher, C.C., III, and Aubry, M., 1995, A revised Cenozoic geochronology and chronostratigraphy: Special Publication - Society for Sedimentary Geology, 54, p. 129-212.

Bird, K. J., 1967, Biostratigraphy of the Tyee Formation (Eocene), southwestern Oregon: Ph.D. dissertation, University of Wisconsin, Madison, 209 p.

Black, G. L., 1990, Geologic map of the Reston quadrangle, Douglas County, Oregon: Oregon Dept. of Geology and Mineral Industries Geologic Map Series GMS-68, scale 1:24,000.

Black, G. L., 1994a, Geologic map of the Kenyon Mountain quadrangle, Douglas and Coos counties, Oregon: Oregon Dept. of Geology and Mineral Industries Geologic Map Series GMS-83, scale 1:24,000.

Black, G. L., 1994b, Geologic map of the Remote quadrangle, Coos County, Oregon: Oregon Dept. of Geology and Mineral Industries Geologic Map Series GMS-84, scale 1:24,000.

Black, G. L. and Priest, G. R., 1993, Geologic map of the Camas Valley quadrangle, Douglas and Coos counties, Oregon: Oregon Dept. of Geology and Mineral Industries Geologic Map Series GMS-76, scale 1:24,000.

Blake, M. C., Jr., 1984, Tectonostratigraphic terranes in southwestern Oregon; *in* Nilsen, T. H., ed., Geology of the Upper Cretaceous Hornbrook Formation, Oregon and

California: Pacific Section, Society of Economic Paleontologists and Mineralogists, v. 42, p. 159-165.

Blake, M. C., Jr., Engebretson, D. C., Jayko, A. S., and Jones, D. L., 1985, Tectono-stratigraphic terranes in southwest Oregon; *in* Howell, D. G., ed., Tectono-stratigraphic terranes of the Circum-Pacific region: Circum-Pacific Council on Energy and Mineral Resources, Earth Science Series, v. 1, p. 145-157.

Brouwers, Elisabeth, Marincovich, Louie, Jr., Ryu, In-Chang, and Niem, Alan, 1995, Paleogeography, paleoecology, and biostratigraphy of upper Paleocene to middle Eocene units of the Tyee basin, southwest Oregon; *in* Fritsche, A. E., ed., 1995, Cenozoic paleogeography of the western United States - II: Pacific Section, SEPM (Society for Sedimentary Geology), book 75, p. 246-256.

Bukry David and Snively, P. D., Jr., 1988, Coccolith zonation for Paleogene strata in the Oregon Coast Range; *in* Filewicz, M. V. and Squires, R. L., eds., Paleogene stratigraphy, west coast of North America: Pacific Section, Society of Economic Paleontologists and Mineralogists, West Coast Paleogene Symposium, v. 58, p. 251-263.

Burchfiel, B. C., Cowan, D. S., Davis, G. A., 1992, Tectonic overview of the Cordilleran orogen in the western United States, *in* Burchfiel, B. C., Lipman, P. W., and Zoback, M. L., eds., The Cordilleran Orogen: Conterminous U.S.: Boulder, Colorado, Geological Society of America, The Geology of North America, v. G-3.

Carayon, Veronique, 1984, Étude géologique de l'extrémité septentrionale de la chaîne des Klamath, sud-ouest Oregon (U.S.A.): Ph.D. dissertation, 3rd Cycle, Pierre and Marie Curie University, University of Paris VI, 186 p., map scale 1:62,500.

Champ, J. G., 1969, Geology of the northern part of the Dixonville quadrangle, Oregon: University of Oregon, Eugene [M.Sc.], 86 p.

Chan, M. A., 1982, Comparison of sedimentology and diagenesis of Eocene rocks, southwest Oregon: Madison, Wisconsin, University of Wisconsin-Madison, Ph.D. dissertation, 322 p.

Chan, M. A. and Dott, R. H., Jr., 1983, Shelf and deep-sea sedimentation in Eocene forearc basin, western Oregon--fan or non-fan?: American Association of Petroleum Geologists Bulletin, v. 67, no. 11, p. 2100-2116.

Clowes, R. M., Brandon, M. T., Green, A. G., Yorath, C. J., Sutherland Brown, A., Kanasewich, E. R., and Spencer, C., 1987, Lithoprobe – southern Vancouver Island: Cenozoic subduction complexes imaged by deep seismic reflections: Canadian Journal of Earth Science, v. 24, no. 1, p. 31-51.

Coleman, R. G., 1972, The Colebrooke Schist of southwestern Oregon and its relation to the tectonic evolution of the region: U.S. Geological Survey Bulletin 1339 61 p.

Coleman, R. G., and Lanphere, M., 1991, The Briggs Creek Amphibolite, Klamath Mountains, Oregon: its origin and dispersal: New Zealand Journal of Geology and Geophysics, v. 34, p. 271-284.

Coleman, R. G., and Lanphere, M. A., 1971, Distribution and age of high-grade blueschists, associated eclogites and amphibolites from Oregon and California: Geological Society of America Bulletin, v. 82, p. 2397-2412.

Cooper, P. A., Kroenke, J. M., and Resig, J. M., 1986, Tectonic implications of seismicity northeast of the Solomon Islands, *in*, Geology and offshore resources of Pacific island arcs – central and western Solomon Islands, eds., Vedder, J. G., Pound, K. S., and Boundy, S. Q., Circum-Pacific Council for Energy and Mineral Resources, v. 4, p. 117-122.

Diehl, J F, Beck, M E, Jr, Beske-Diehl, S, Jacobson, D, Hearn, B C, Jr, 1983, Paleomagnetism of the Late Cretaceous-early Tertiary north-central Montana alkalic province: Journal of Geophysical Research, v.88, p.10593-10609.

Diller, J. S., 1898, Roseburg folio: U.S. Geological Survey Geologic Atlas of the United States, Folio No. 49.

Dott, R. H., 1965, Mesozoic-Cenozoic tectonic history of the southern Oregon Coast in relation to Cordilleran orogenesis: Journal of Geophysical Research, v. 70, p. 4687-4707.

Duncan, R. A., 1982, A captured island chain in the Coast Range of Oregon and Washington: Journal of Geophysical Research, v. 87, p. 10,827-10,837.

Elphic, L. G., 1969, Geology of the southern one-third of the Glide quadrangle, Oregon: unpublished master's thesis, University of Oregon, Eugene, 78 p.

Engelbreton, D. C., Gordon, R.G., and Cox., A., 1985, Relative motions between oceanic and continental plates in the Pacific basin: Geological Society of America Special Paper, v. 206, 59p.

England, P. C., and Wells, R. E., 1991, Neogene rotations and continuum deformation of the Pacific Northwest convergent margin: Geology, v. 19, p. 978-981.

Fairchild, R. W., 1966, Geology of T. 29 S., R. 11 W. in the Sitkum and Coquille quadrangles, Coos County, Oregon: unpublished master's thesis, University of Oregon, Eugene, 68 p.

Fisher, R. A., 1953, Dispersion on a sphere: Proceedings – Royal Society of London, v. A217, p. 295-305.

Garcia, M. O., 1979, Petrology of the Rogue and Galice Formations, Klamath Mountains, Oregon: Identification of a Jurassic Island Arc sequence: *Journal of Geology*, v. 86, p. 29-41.

Garcia, M. O., 1982, Petrology of the Rogue River island arc complex, southwest Oregon: *American Journal of Science*, v. 282, p. 783-807.

Gautier, D. L. and Varnes, K. L., 1993, Plays for assessment in Region II, Pacific Coast as of October 4, 1993: 1995 National Assessment of oil and gas: U.S. Geological Survey Open-File Report 93-596-B, 11p.

Hampton, E. R., 1958, Geology of the southeast one-quarter of the Tyee quadrangle and part of the adjacent Sutherlin quadrangle, Oregon: unpublished master's thesis, Oregon State College, Corvallis, 55 p.

Harms, J. E., 1957, Geology of the southeast one-quarter of the Camas Valley quadrangle, Douglas County, Oregon: master's thesis, Oregon State University, Corvallis, 70 p.

Harper, G. D., and Wright, J. E., 1984, Middle to Late Jurassic tectonic evolution of the Klamath Mountains, California-Oregon: *Tectonics*, v. 3, p. 759-772.

Haq, Z. N., 1975, Geology of the northwest quarter of Roseburg quadrangle, Douglas County, Oregon, U.S.A.: unpublished master's thesis, University of Oregon, Eugene, 75 p.

Heller, P. L. and Dickinson, W. R., 1985, Submarine ramp facies model for delta-fed, sand-rich turbidite systems: *American Association of Petroleum Geologists Bulletin*, v. 69, no. 6, p. 960-976.

Heller, P. L. and Ryberg, P. T., 1983, Sedimentary record of subduction to forearc transition in the rotated Eocene basin of western Oregon: *Geology*, v. 11, no. 7, p. 380-383.

Heller, P. L., Peterman, Z. E., O'Neill, J. R., and Shafiqullah, M., 1985, Isotopic provenance of sandstones from the Eocene Tyee Formation, Oregon Coast Range: *Geological Society of America Bulletin*, v. 96, p. 770-780.

Hicks, D. L., 1964, Geology of the southwest quarter of the Roseburg quadrangle, Oregon: master's thesis, University of Oregon, Eugene, 65 p.

Hixson, H. C., 1965, Geology of the southwest quarter of the Dixonville quadrangle, Oregon: University of Oregon, Eugene [M.Sc.], 97 p.

Hotz, P. E., 1971, Plutonic rocks of the Klamath Mountains, California and Oregon: U.S. Geological Survey Professional Paper 684-B 1-20 p.

Hoover, Linn, 1963, Geology of the Anlauf and Drain quadrangles, Douglas and Lane counties, Oregon: U.S. Geological Survey Bulletin 1122-D, 62 p.

Imlay, R. W., Dole, H. M., Wells, F. G., and Peck, D. L., 1959, Relations of certain Jurassic and Lower Cretaceous formations in southwestern Oregon: American Association of Petroleum Geologists, v. 43, p. 2770-2785.

Irwin, W. P., 1964, Late Mesozoic orogenies in the ultramafic belts of northwestern California and south western Oregon: U.S. Geological Survey Professional Paper 501-C 501-C, 1-9 p.

Jayko, A. S., 1996a, Reconnaissance geologic map of the Lane Mountain 7.5 minute quadrangle, Oregon, Open-File Report - U. S. Geological Survey, OF 95-0020, p. 14 (1 sheet), sect., 26 refs.

Jayko, A. S., 1996b, Reconnaissance geologic map of the White Rock 7.5 minute quadrangle, Oregon: Open-File Report - U. S. Geological Survey, OF 95-0018, p. 13 (1 sheet), sect., 21 refs.

Jayko, A. S., 1997, Reconnaissance geologic map of the Dodson Butte 7.5' quadrangle, Oregon: Open-File Report - U. S. Geological Survey, OF 97-0514, p. 12 (1 sheet), illus. incl. sect., 26 refs.

Jayko, A. S. and Gallagher, M., 1997, Reconnaissance geologic map of the Myrtle Creek 7.5' quadrangle, Oregon: Open-File Report - U. S. Geological Survey, OF 97-0527, p. 10 (1 sheet), 27 refs.

Jayko, A. S. and Wells, R. E., in press, Reconnaissance geologic map of the Dixonville 7.5' quadrangle, Oregon: Open-File Report - U. S. Geological Survey.

Johnson, W. R., 1965, Structure and stratigraphy of the southeastern quarter of the Roseburg 15-minute quadrangle, Douglas County, Oregon: master's thesis, University of Oregon, Eugene, 85 p.

Kroenke, L. W., 1984, Cenozoic tectonic development of the southwest Pacific: United Nations ESCAP, CCOP/SOPAC Technical Bulletin 6, 122p.

Kroenke, L.W., 1989, Interpretation of a multichannel seismic reflection profile northeast of the Solomon Islands, from the southern flank of the Ontong Java Plateau across the Malaita anticlinorium to the Solomon islands arc: in Vedder, J. G., and Bruns, T. R., eds., Geology and offshore resources of Pacific island arcs – Solomon Islands and Bougainville, Papua New Guinea Regions: Houston Texas, Circum-Pacific Council for Energy and Mineral Resources Earth Science Series, v. 12, p. 145-148.

Koler, T. E., 1979, Stratigraphy and sedimentary petrology of the northwest quarter of the Dutchman Butte quadrangle, southwest Oregon: Portland, OR, Portland State University, unpublished master's thesis, 72 p.

Kugler, R. L., 1979, Stratigraphy and petrology of the Bushnell Rock Member of the Lookingglass Formation, southwestern Oregon Coast Range: Eugene, OR, University of Oregon, unpublished master's thesis, 118 p.

Kvenvolden, K. A., Lorenson, T. D., and Niem, A. R., 1995, Natural hydrocarbon gases in the Coast Range of southern Oregon: U.S. Geological Survey Open-File Report 95-93, 19 p.

Lane, J. W., 1988, Relations between geology and mass movement features in a part of the East Fork Coquille River watershed, southern Coast Range, Oregon: master's thesis, Oregon State University, Corvallis, 107 p.

Lawrence, J. K., 1969, Geology of the southern third of the Sutherlin quadrangle, Oregon: unpublished master's thesis, University of Oregon, Eugene, 100 p.

Magoon, L. B., 1966, Geology of T. 28 S., R. 11 W. of the Coquille and Sitkum quadrangles, Oregon: unpublished master's thesis, University of Oregon, Eugene, 73 p.

McKnight, Brian K., 1971, Petrology and sedimentation of Cretaceous and Eocene rocks in the Medford-Ashland region, southwestern Oregon: Corvallis, OR, Oregon State University, Ph.D. dissertation, 177 p.

Miles, G. A., 1977, Planktonic Foraminifera of the lower Tertiary Roseburg, Lookingglass, and Flourney formations, southwest Oregon: Ph.D. dissertation, University of Oregon, Eugene, 374 p.

Miyashiro, A., 1978, A chemical classification of volcanic rocks based on the total alkali-silica diagram; *Journal of petrology*, v. 27, p. 745-750.

Molenaar, C. M., 1985, Depositional relations of Umpqua and Tyee formations (Eocene), southwestern Oregon: *American Association of Petroleum Geologists Bulletin*, v. 69, no. 8, p. 1217-1229.

Moore, J. F., Jr., 1957, Geology of the northeast quarter of Camas Valley quadrangle, Douglas County, Oregon: unpublished master's thesis, Oregon State College, Corvallis, 95 p.

Mutti, Emiliano and Ricci Lucchi, F., 1972, Le torbiditi dell'Appennino settentrionale: introduzione all'analisi di facies: *Memorie della Societa Geologica Italiana*, v. 11, p. 161-199 -- translated by T. H. Nilsen, 1978, Turbidites of the northern Appenines: introduction to facies analysis: *International Geology Review*, v. 20,

p. 125-166.

Nelson, E. B., 1966, The geology of the Fairview-McKinley area, central Coos County, Oregon, unpublished master's thesis, University of Oregon, Eugene, 63 p.

Niem, A. R. and Niem, W. A., 1990, Geology and oil, gas, and coal resources, southern Tyee basin, southern Coast Range, Oregon: Oregon Dept. of Geology and Mineral Industries, Open-File Report O-89-3, 11 tables, 3 plates, 44 p.

Niem, W. A., Niem, A. R., and Snively, P. D., Jr., 1992c, Late Cenozoic continental margin of the Pacific Northwest -- Sedimentary embayments of the Washington-Oregon coast; *in* Burchfiel, B. C., Lipman, P. W., and Zoback, M. L., eds., The Cordilleran Orogen: Conterminous U.S.: Geological Society of America The Geology of North America, volume G-3, p.314-319.

Olmstead, D. L., 1989, Hydrocarbon exploration and occurrences in Oregon: Oregon Dept. of Geology and Mineral Industries Oil and Gas Investigation 15, 78p.

Patterson, P. V., 1961, Geology of the northern third of the Glide quadrangle, Oregon: master's thesis, University of Oregon, Eugene, 83 p.

Payton, C. C., 1961, The geology of the middle third of the Sutherlin quadrangle, Oregon: master's thesis, University of Oregon, Eugene, 81 p.

Peck, D. L., Griggs, A. B., Schlicker, H. G., Wells, F. G., and Dole, H. M., 1964, Geology of central and northern parts of the western Cascade Range in Oregon: U.S. Geological Survey Professional Paper 449 449, 56 p.

Personius, S. F., 1993, Age and origin of fluvial terraces in the central Coast Range, western Oregon: U.S. Geological Survey Bulletin 2038, 56 p.

Perttu, R. K. and Benson, G. T., 1980, Deposition and deformation of the Eocene Umpqua Group, Sutherlin area, southwestern Oregon: Oregon Geology, v. 42, no. 8, p. 135-140.

Peterson, N. V., 1957, The geology of the southeast third of the Camas Valley quadrangle, Oregon: Eugene, University of Oregon, M.S. thesis, 89 p.

Pyle, D. G., 1988, Geochemical evolution of the Roseburg Formation basaltic rocks, southern Oregon Coast Range: Corvallis, Oregon, Oregon State University master's thesis, 137 p.

Ramp, Len, 1972, Geology and mineral resources of Douglas County, Oregon: Oregon Dept. of Geology and Mineral Industries Bulletin 75, 106 p.

Roure, F., and Blanchet, R., 1983, A geologic transect between the Klamath Mountains and the Pacific Ocean, southwestern Oregon: a model for paleosubduction: *Tectonophysics*, v. 91, p. 53-71.

Ryberg, P. T., 1984, Sedimentation, structure, and tectonics of the Umpqua Group (Paleocene to early Eocene), southwestern Oregon: Tucson, Arizona, University of Arizona, Ph.D. dissertation, 280 p.

Ryu, In-Chang, 1995, Stratigraphy, sedimentology, and hydrocarbon potential of the lower to middle Eocene forearc and subduction zone strata in the southern Tyee basin, Oregon Coast Range: Corvallis, OR, Oregon State University, Ph.D. dissertation.

Ryu, In-Chang, Niem, A. R., and Niem, W. A., 1992, Schematic fence diagram of the southern Tyee basin, Oregon Coast Range, showing stratigraphic relationships of exploration wells to surface measured sections: Oregon Dept. of Geology and Mineral Industries Oil and Gas Investigation 18, 28 p., 1 oversized sheet.

Ryu, In-Chang, Niem, A. R., and Niem, W. A., 1996, Oil and gas potential of the southern Tyee basin, southern Oregon Coast Range: Oregon Department of Geology and Mineral Industries Oil and Gas Investigation 19, 141 p.

Sanborn, E. I., 1937, The Comstock flora of west central Oregon; Eocene flora of western America: Carnegie Institute of Washington Publication 465, p. 1-28.

Saleeby, J. B., Harper, G. D., Snoke, A. W., and Sharp, W. D., 1982, Time relations and structural-stratigraphic patterns in ophiolite accretion, west central Klamath Mountains, California: *Journal of Geophysical Research*, v. 87, p. 3831-3848.

Seeley, W. O., 1974, Geology of the southeastern Dixonville quadrangle, Oregon: University of Oregon, Eugene [M.Sc.], 77 p.

Simpson, R. W. and Cox, A., 1977, Paleomagnetic evidence for tectonic rotation of the Oregon Coast Range: *Geology*, v. 5, p. 585-589.

Smith, J. G., Page, N. J., Johnson, M. G., Moring, B. C., and Gray, F., 1982, Preliminary geologic map of the Medford 1 degree by 2 degree quadrangle, Oregon: U. S. Geological Survey Open-File Report 82-955, scale 1:250,000.

Snively, P. D., Jr., 1984, Sixty million years of growth along the Oregon continental margin; *in* Clarke, S. H., ed., Highlights in marine research: U.S. Geological Survey Circular 938, p. 9-18.

Snively, P. D., Jr., 1987, Tertiary geologic framework, neotectonics, and petroleum potential of the Oregon-Washington continental margin; *in* Scholl, D. W., Grantz, A., and Vedder, J. G., eds., Geology and resource potential of the continental margin of western North America and adjacent ocean basins--Beaufort Sea to Baja California:

Circum-Pacific Council for Energy and Mineral Resources Earth Science Series, v. 6, p. 305-335.

Snively, P. D., Jr., N. S., MacLeod, and H. C., Wagner, 1968, Tholeiitic and alkalic basalts of the Eocene Siletz River Volcanics, Oregon Coast Range: American Journal of Science, v. 266, p. 454-481.

Snively, P. D., Jr., Wagner, H. C., and MacLeod, N. S., 1964, Rhythmic-bedded eugeosynclinal deposits of the Tyee Formation, Oregon Coast Range: Kansas Geological Survey, Bulletin 169, p. 461-480.

Thompson, R. L., 1968, The geology of the middle one-third of the Glide quadrangle, Oregon: master's thesis, University of Oregon, Eugene, 57 p.

Thoms, R. E., 1965, Biostratigraphy of the Umpqua Formation, southwest Oregon: Ph.D. dissertation, University of California, Berkeley, 219 p.

Trehu, A. M., Asudeh, I., Brocher, T. M., Luetgert, J. H., Mooney, W. D., Nabelek, J. L., Nakamura, Y., 1994, Crustal architecture of the cascadia forearc: Science, v. 265, p. 237-243.

Trigger, J. K., 1966, Geology of the south-central part of the Sitkum quadrangle, Coos County, Oregon: unpublished master's thesis, University of Oregon, Eugene, 79 p.

Turner, F. E., 1938, Stratigraphy and Mollusca of the Eocene of western Oregon: Geological Society of America Special Paper 10, 130p.

U. S. Geological Survey, 1996, Aeromagnetic Map of the Roseburg area on parts of the Roseburg, Coos Bay, Medford, and Cape Blanco 1 x 2° Quadrangles, Oregon: U. S. Geological Survey Open File Report OF96-695 scale 1:100,000.

Walker, G. W. and MacLeod, N. S., 1991, Geologic map of Oregon: U.S. Geological Survey, scale 1:1,500,000.

Walker, R. G., and Mutti, Emiliano, 1973, Turbidite facies and facies associations, *in* Middleton, G. V. and Bouma, A. H., eds., Turbidites and deep-water sedimentation: Pacific Section, Society of Economic Paleontologists and Mineralogists, Short Course (Anaheim, 1973), p. 119-157.

Weatherby, D. G., 1991, Stratigraphy and sedimentology of the late Eocene Bateman Formation, southern Oregon Coast Range: Eugene, OR, University of Oregon, M.S. thesis, 161 p.

Wells, F. G. and Peck, D. L., 1961, Geologic map of Oregon west of the 121st meridian: U.S. Geological Survey Miscellaneous Geologic Investigations Map I-325, scale 1:500,000.

Wells, F. G. and Waters, A. C., 1934, Quicksilver deposits of southwestern Oregon: U.S. Geological Survey Bulletin 850, 58 p.

Wells, R. E., 1989, Mechanisms of Cenozoic tectonic rotation, Pacific Northwest convergent margin, U.S.A.: *in* Kiessel, C. and Laj, C., Paleomagnetic rotations and continental deformation, NATO Advanced Study Institute v. C254, p. 313-325, Kluwer Publishers, Netherlands.

Wells, R. E., and Coe, R. S., 1985, Paleomagnetism and geology of Eocene volcanic rocks of southwest Washington, implications for mechanisms of tectonic rotation: *Journal of Geophysical Research*, v. 90, p. 1925-1947

Wells, R. E., Engebretson, D. C., Snavely, P. D., Jr., and Coe, R. S., 1984, Cenozoic plate motions and the volcano-tectonic evolution of western Oregon and Washington: *Tectonics*, v. 3, no. 2, p. 275-294.

Wells, R. E. and Heller, P. L., 1988, The relative contribution of accretion, shear, and extension to Cenozoic tectonic rotation in the Pacific Northwest: *Geological Society of America Bulletin*, v. 100, p. 325-338.

Wells, R. E., Kelly, M. M., Levi, S., Schultz, K., and McElwee, K., 1985, Folding and rotation of Paleocene pillow basalt near Roseburg, Oregon: *Eos*, (American Geophysical Union Transactions), v. 66, p. 863.

Wells, R. E., Weaver, C. S., Blakely, R. J., 1998, Fore-arc migration in Cascadia and its neotectonic significance, *Geology*, v. 26, no. 8, p. 759-762.

Westhusing, J. K., 1959, The geology of the northern third of the Sutherlin quadrangle, Oregon: master's thesis, University of Oregon, Eugene, 111 p.

Wiley, T. J., 1995, Reconnaissance geologic map of the Dora and Sitkum quadrangles, Coos County, Oregon: Oregon Department of Geology and Mineral Industries Geological Map Series GMS-98, scale 1:24,000.

Wiley, T. J. and Black, G. L., 1994, Geologic map of the Tenmile quadrangle, Douglas County, Oregon: Oregon Dept. of Geology and Mineral Industries: Geologic Map Series GMS-86, scale 1:24,000.

Wiley, T. J., Priest, G.R., and Black, G. L., 1994, Geologic map of the Mt. Gurney quadrangle, Douglas and Coos counties, Oregon: Oregon Dept. of Geology and Mineral Industries: Geologic Map Series GMS-85, scale 1:24,000.

LIST OF TABLES

- Table 1. Oil and Gas exploration wells (also on Sheet 2).
- Table 2. Paleontology
a) Coccoliths and Foraminifera
b) Macrofossils
c) Fossil Index
- Table 3. Paleomagnetism of the Siletz River Volcanics and Tyee Basin
- Table 4. Chemistry of the Siletz River Volcanics, most flows are alkalic, based on the criteria of Miyashiro (1978)

LIST OF FIGURES

- Figure 1 Location of Roseburg 30' X 60' Quadrangle (figure also on sheet 2)
- Figure 2 Generalized geologic and tectonic features of the Roseburg Quadrangle showing oil and gas exploration wells from Table 1 (figure also on sheet 2).
- Figure 3 Sources of Geologic Mapping a) this project; b) Consulted extensively (figure also on sheet 2).
- Figure 4 Time – rock chart for the Tertiary strata of the Tyee basin.
- Figure 5 Coccolith and Foraminifera localities listed in Table 2a.
- Figure 6 Macrofossil localities listed in Table 2b.
- Figure 7 Paleomagnetic sites and location of chemistry samples listed in Tables 3 and 4.
- Figure 8 Northwest-southeast tectonic cross section of the Roseburg area, showing hypothetical deep crustal structure created by Eocene obduction of the Siletz terrane onto the continental margin.
- Figure 9 Paleomagnetism of the Siletz River Volcanics (SRV) shows clockwise rotation. a) stereoplot of reversed magnetization directions, showing a_{95} confidence limits and 79° clockwise rotation of SRV mean direction from the Paleocene reference direction for North America (Diehl and others, 1983); b and c) typical alternating field demagnetization plots. Characteristic component isolated between 20 and 50 nT.
- Figure 10. Early Eocene continental margin in Pacific Northwest. Reconstruction based on pre-rotation trend of Umpqua fold and thrust belt and other pre-Tyee folds in Siletz River Volcanics and Crescent Formation of the Coast Range (Wells and Coe, 1985; Wells, 1989). Folds are inferred to be the result of deformation of the Siletz terrane against the pre-Tertiary margin, as observed in the Roseburg quadrangle.

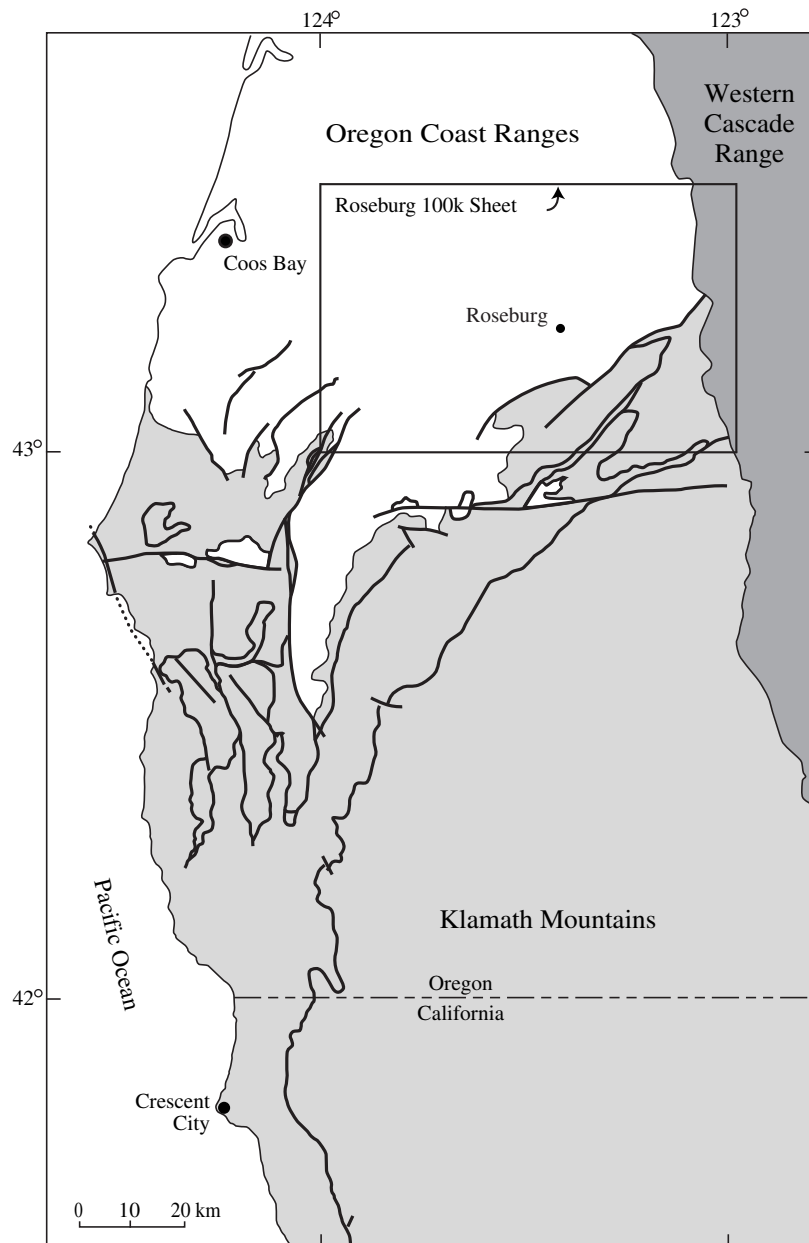


Figure 1. Location Map modified from Ryberg (1984) and Coleman and Lanphere (1991)

EXPLANATION

- Western Cascade Range (Eocene, Oligocene, and Miocene)
- Oregon Coast Ranges (Paleocene and Eocene)
- Klamath Mountains (Mesozoic)
- Contact
- Fault

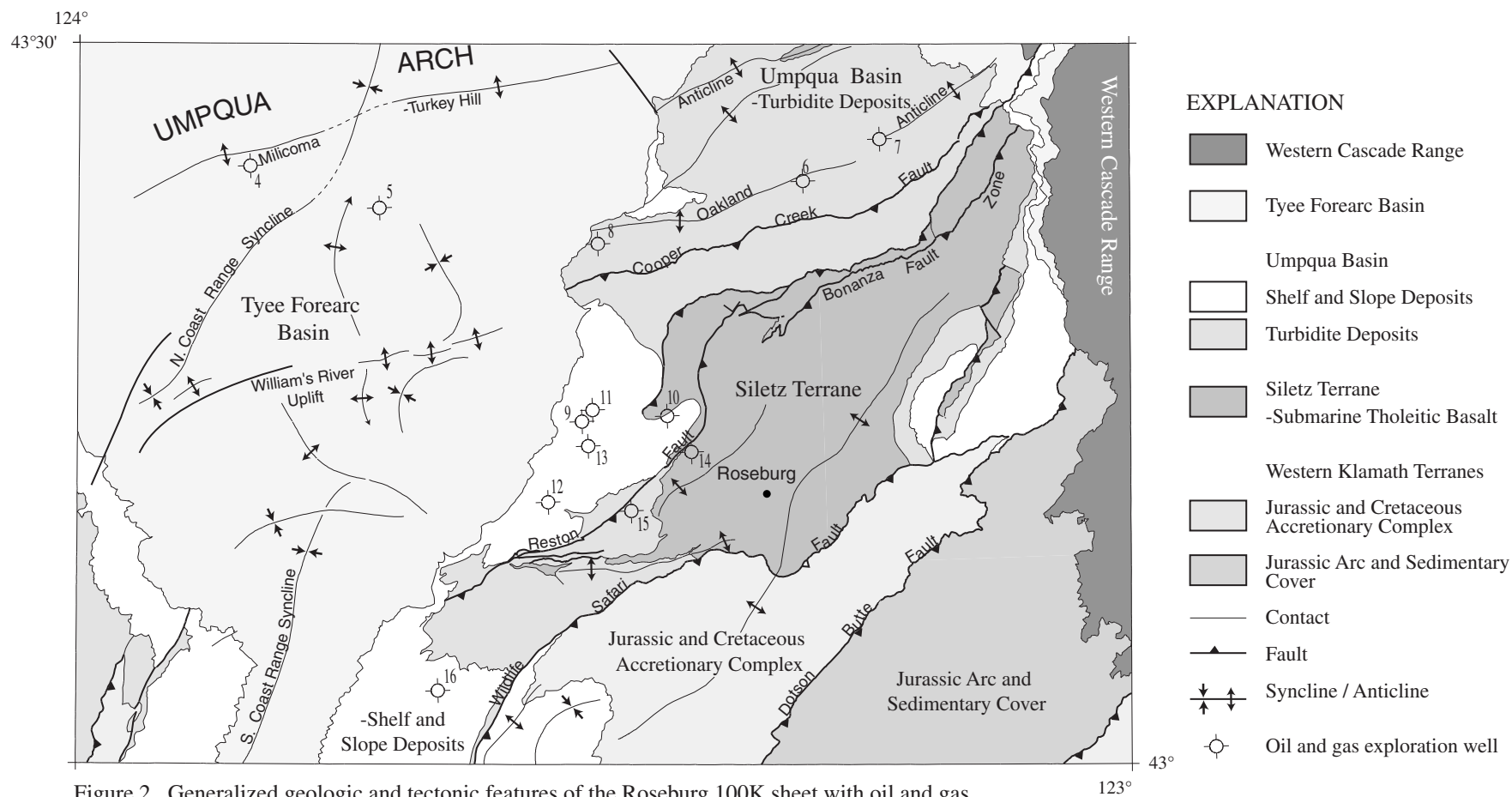


Figure 2. Generalized geologic and tectonic features of the Roseburg 100K sheet with oil and gas exploration wells from Table 1.

Table 1. Oil and gas exploration wells

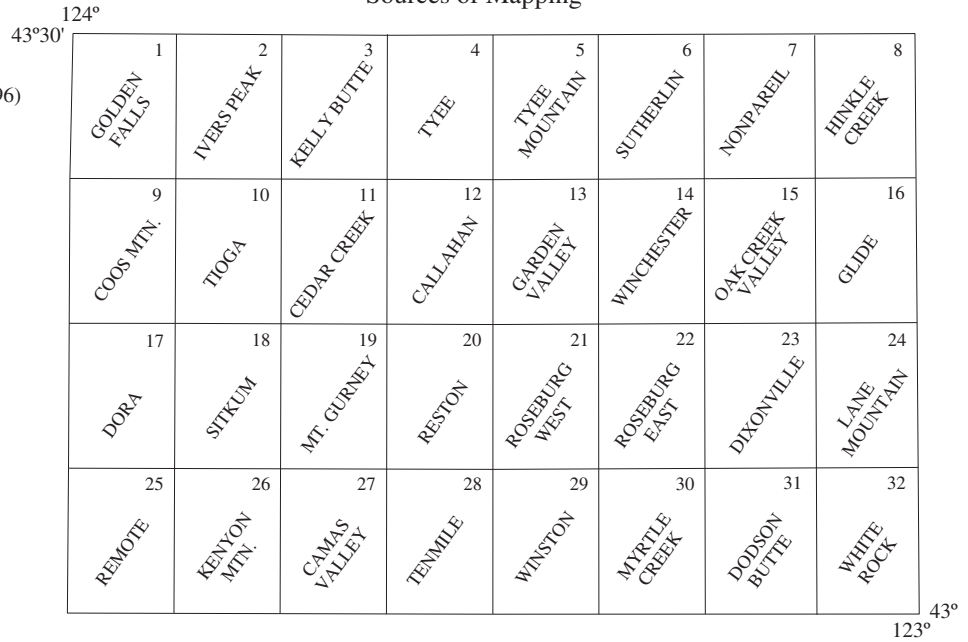
#	Well Name	Well Depth(ft)	Latitude	Longitude
4	Amoco_Weyerhaeuser_F-1	4,428	43.406	123.837
5	Amoco_Weyerhaeuser_B-1	11,330	43.386	123.714
6	Sheldon_C._Clark_"Oakland_well"	2,235	43.405	123.311
7	Mobil_Oil_Corp._Sutherlin_Unit_1	13,177	43.434	123.238
8	Union_Oil_Co._Liles_1	7,002	43.362	123.506
9	Hutchins._&_Marrs_Glory_Hole_1	2,987	43.238	123.521
10	Community_Oil_&_Gas_Co._Scott_1	3,693	43.242	123.440
11	Diamond_Drill_Contracting_Co._Hamilton_Ranch_Well_3	545	43.246	123.511
12	Diamond_Drill_Contracting_Co._Hamilton_Ranch_Well_1	628	43.182	123.553
13	Diamond_Drill_Contracting_Co._Hamilton_Ranch_Well_2	1,109	43.221	123.515
14	W._F._Kernin_Well_1	3,900	43.217	123.417
15	F._W._Dillard_unnamed	700	43.176	123.474
16	Uranium_Oil_&_Gas_Co._Ziedrich_1	4,368	43.051	123.657

well number from Niem and Niem (1990)

Sources of Mapping

Figure 3a.

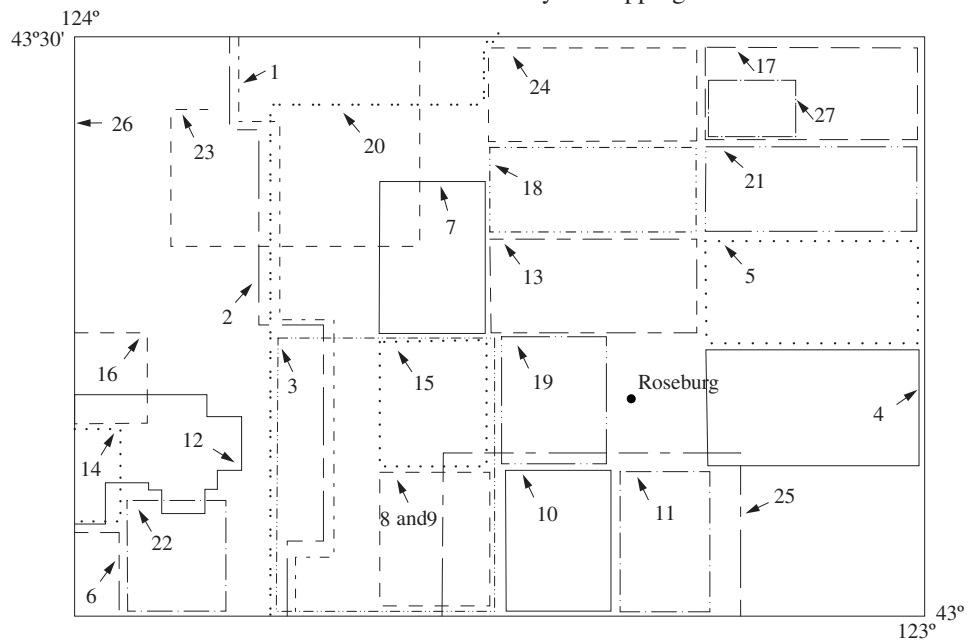
- 1 Molenaar, Black, Wells (1996)
- 2 Molenaar, Black, Wells, Wheeler (1996)
- 3 Baldwin, unpublished, Wells
- 4 Baldwin, unpublished, Wells
- 5 Wells, 1994 mapping
- 6 Wells, 1994 mapping
- 7 Wells, 1994 mapping
- 8 Wells, 1995 mapping
- 9 Molenaar, Black, Wells (1996)
- 10 Wells, Molenaar and Black (1996)
- 11 Wells, 1995 mapping
- 12 Wells and Smith, 1994 mapping
- 13 Felger, Abolins, and Wells (1992)
- 14 Wells, 1992 mapping
- 15 Wells, 1993 mapping
- 16 Wells and Niem, 1995 mapping
- 17 Wiley (1995)
- 18 Wiley (1995)
- 19 Wiley, Priest and Black (1994)
- 20 Black (1990)
- 21 Wells, 1990-1991 mapping
- 22 Wells, 1990-1991 mapping
- 23 Jayko and Wells (1999)
- 24 Jayko (1996)
- 25 Black (1995)
- 26 Black (1994)
- 27 Black and Priest (1993)
- 28 Black (1990)
- 29 Jayko (unpublished mapping)
- 30 Jayko and Gallagher (1997)
- 31 Jayko (1997)
- 32 Jayko (1996)

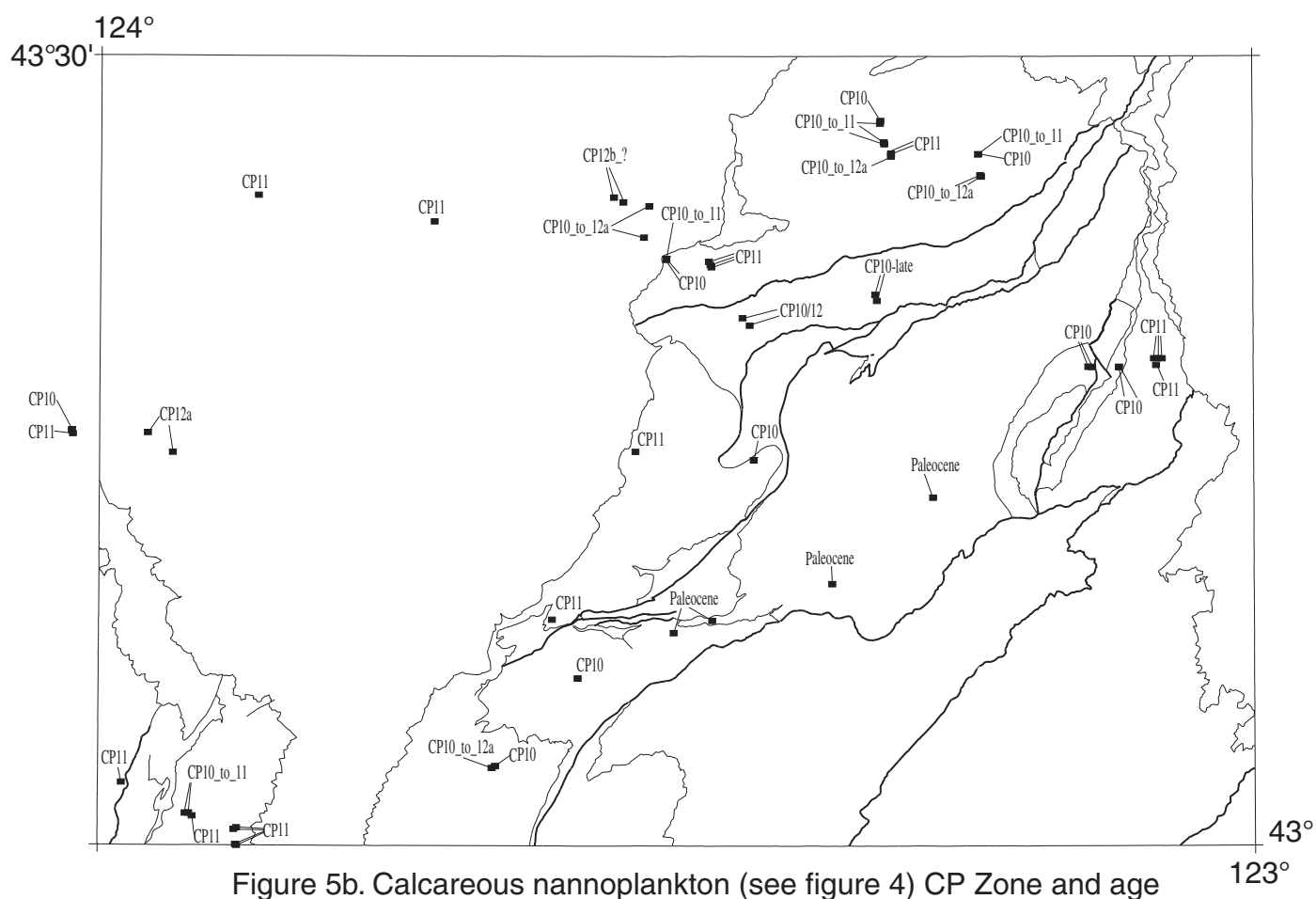
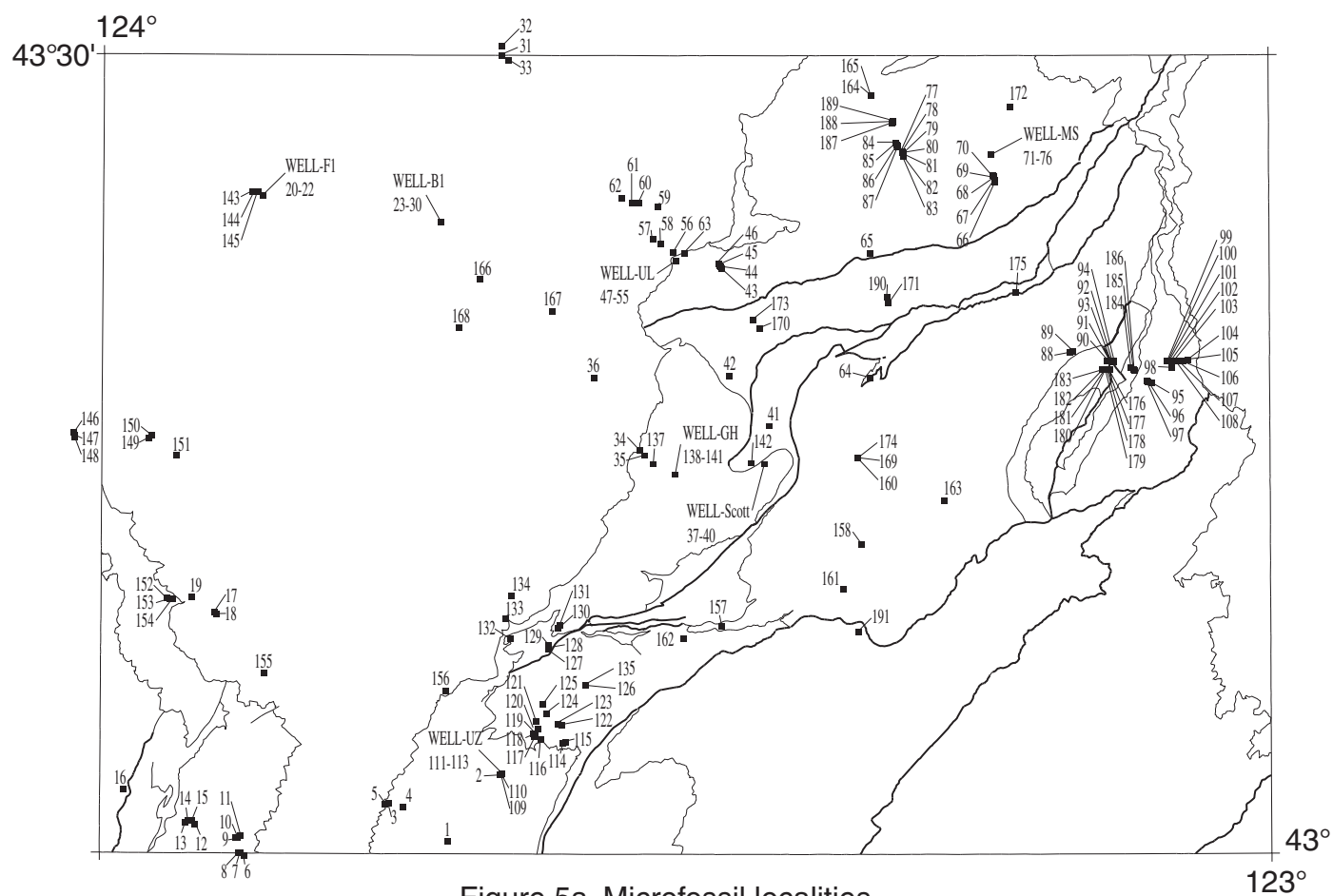


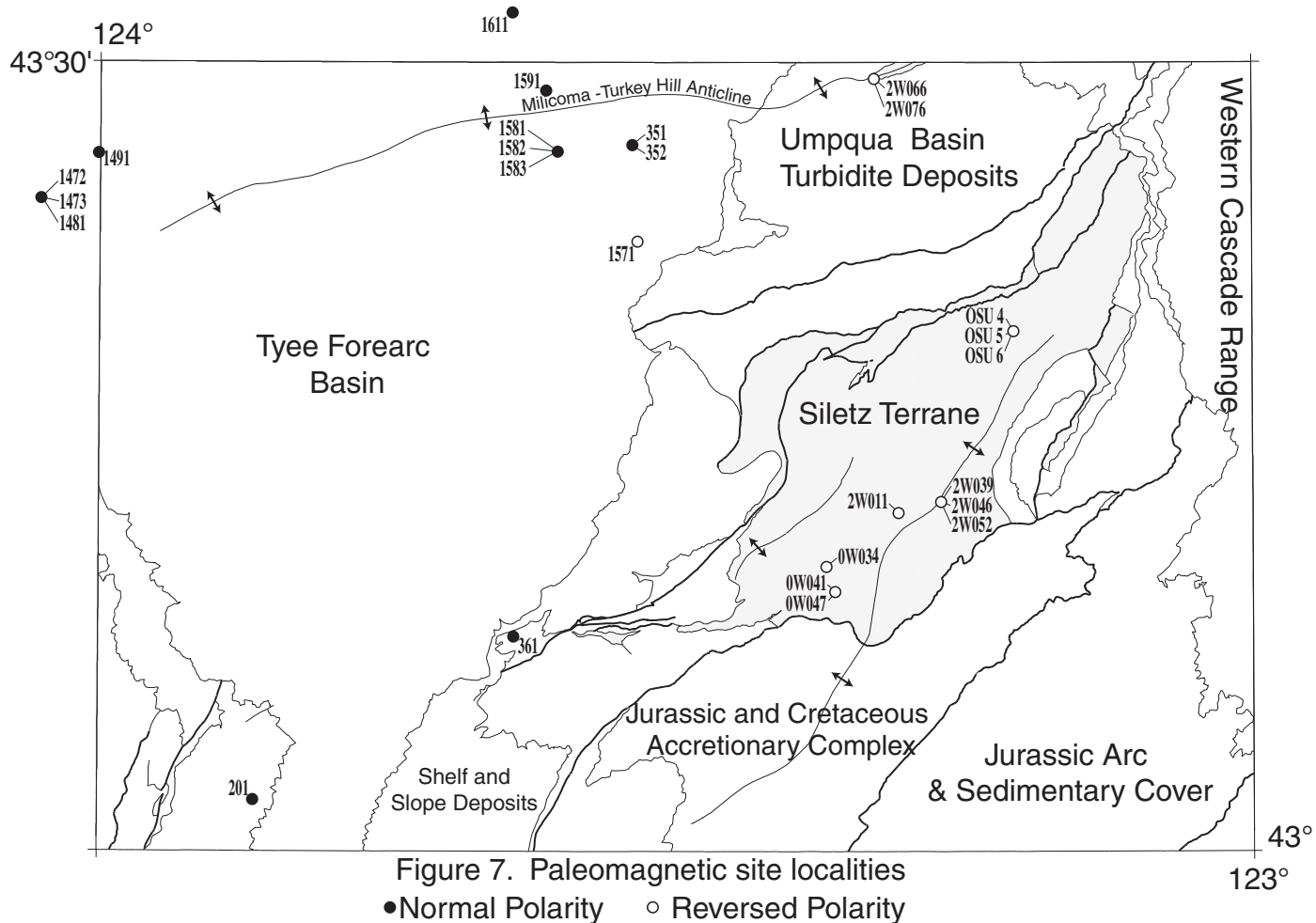
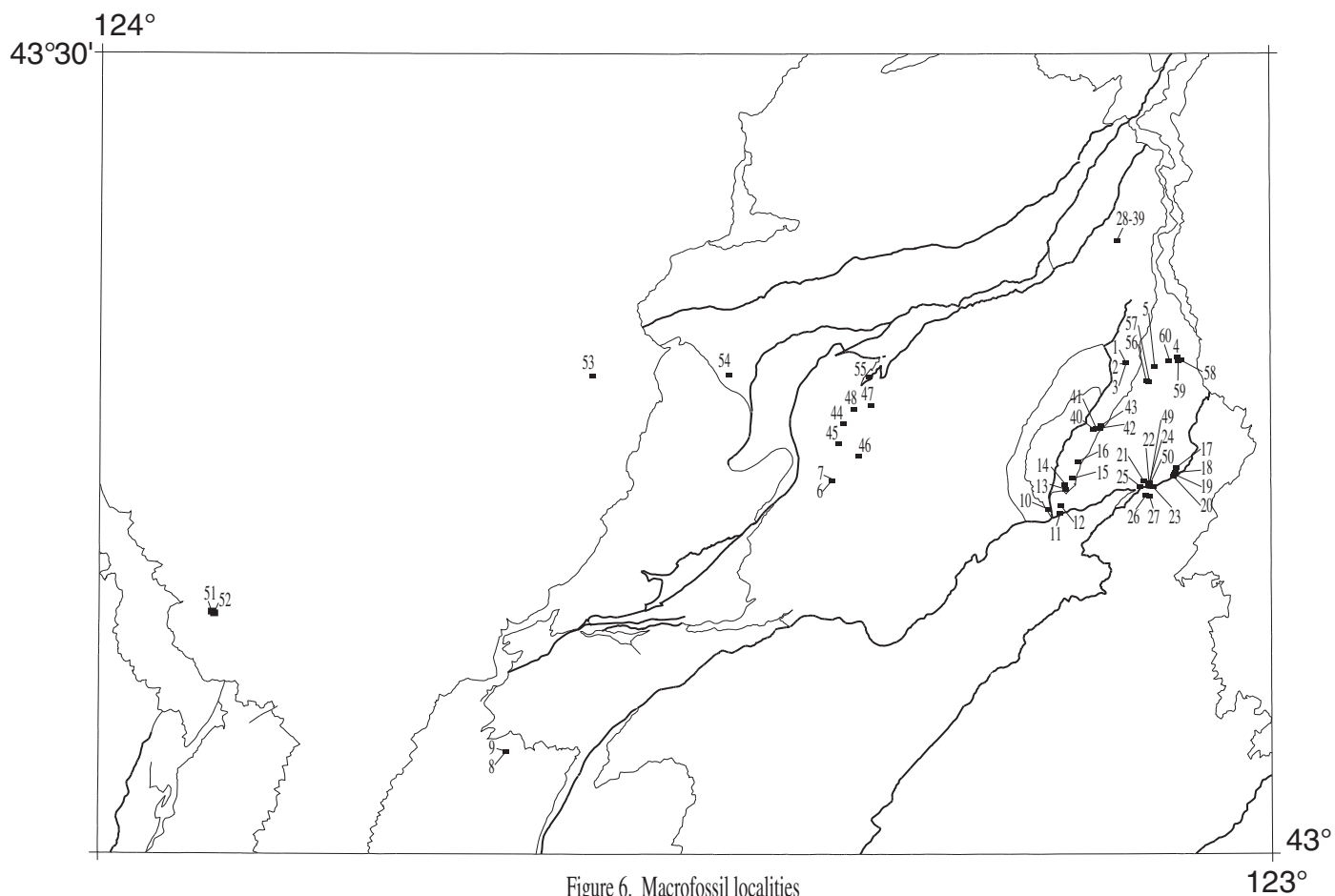
Sources Consulted Extensively in Mapping

Figure 3b.

- 1 Baldwin (1961)
- 2 Baldwin and Beaulieu (1973)
- 3 Baldwin and Perttu (1989)
- 4 Champ (1969)
- 5 Elphic (1969)
- 6 Fairchild (1966)
- 7 Hampton (1958)
- 8 Haq (1975)
- 9 Harms (1957)
- 10 Hicks (1964)
- 11 Johnson (1965)
- 12 Lane (1988)
- 13 Lawrence (1961)
- 14 Magoon (1966)
- 15 Moore (1957)
- 16 Nelson (1966)
- 17 Patterson (1961)
- 18 Payton (1961)
- 19 Peterson (1957)
- 20 Ryberg (1984)
- 21 Thompson (1968)
- 21 Trigger (1966)
- 23 Weatherby, (1991)
- 24 Westhusing (1959)
- 25 Carayon (1984)
- 26 Diller (1898)
- 27 Wells and Waters (1934)







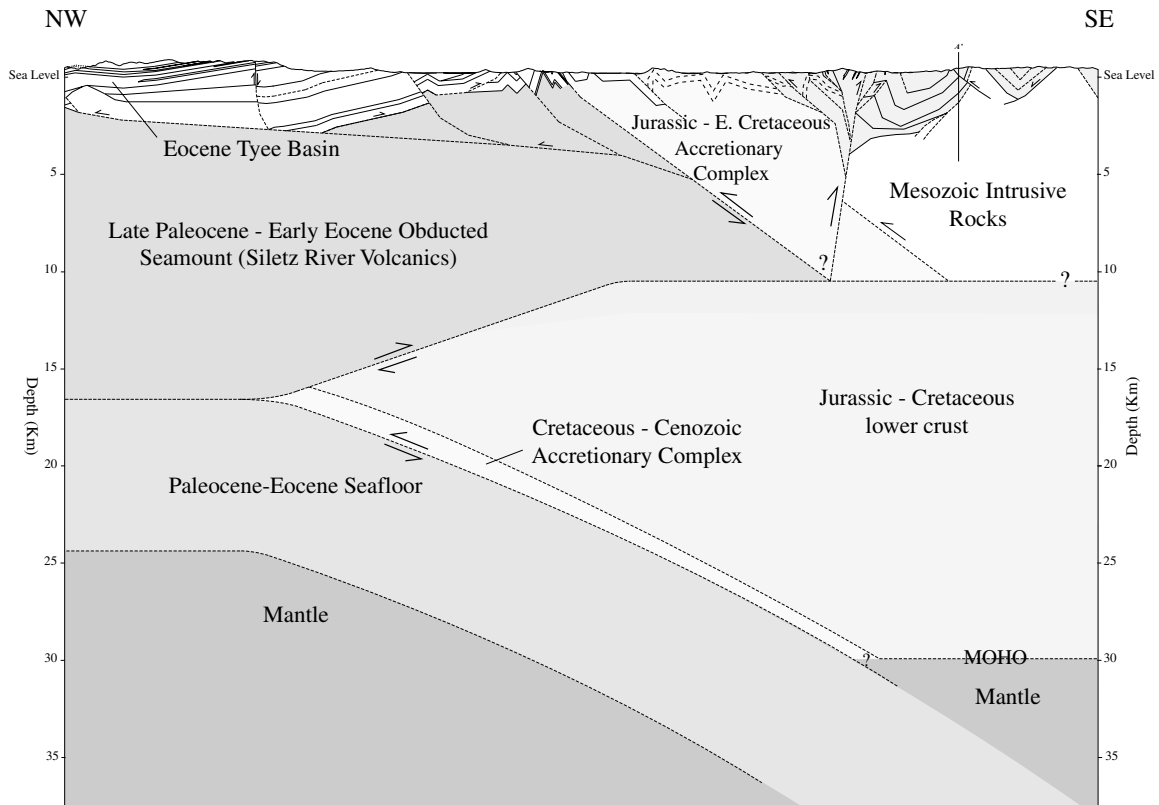


Figure 8.

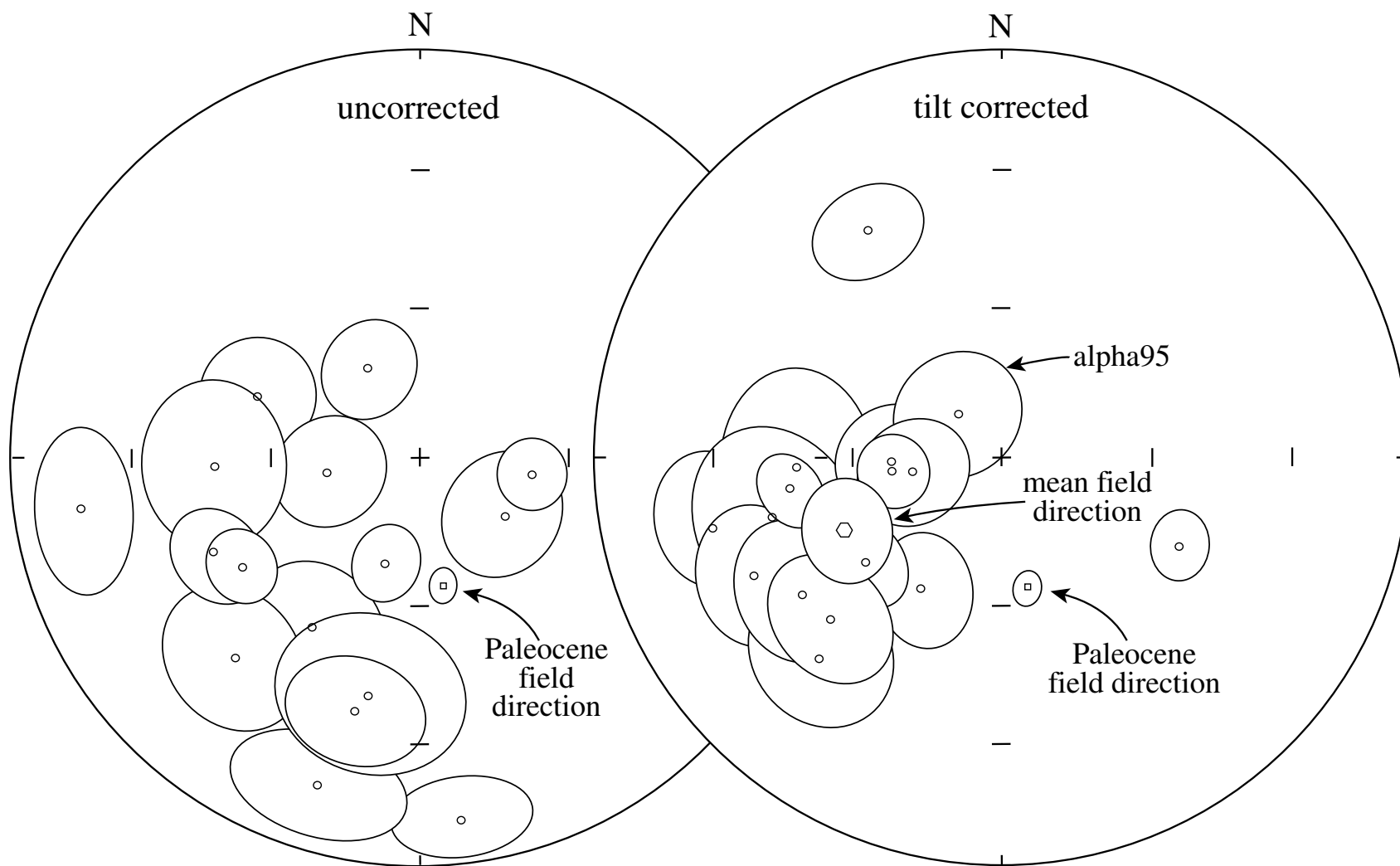


Figure 9a.

Figure 9b.

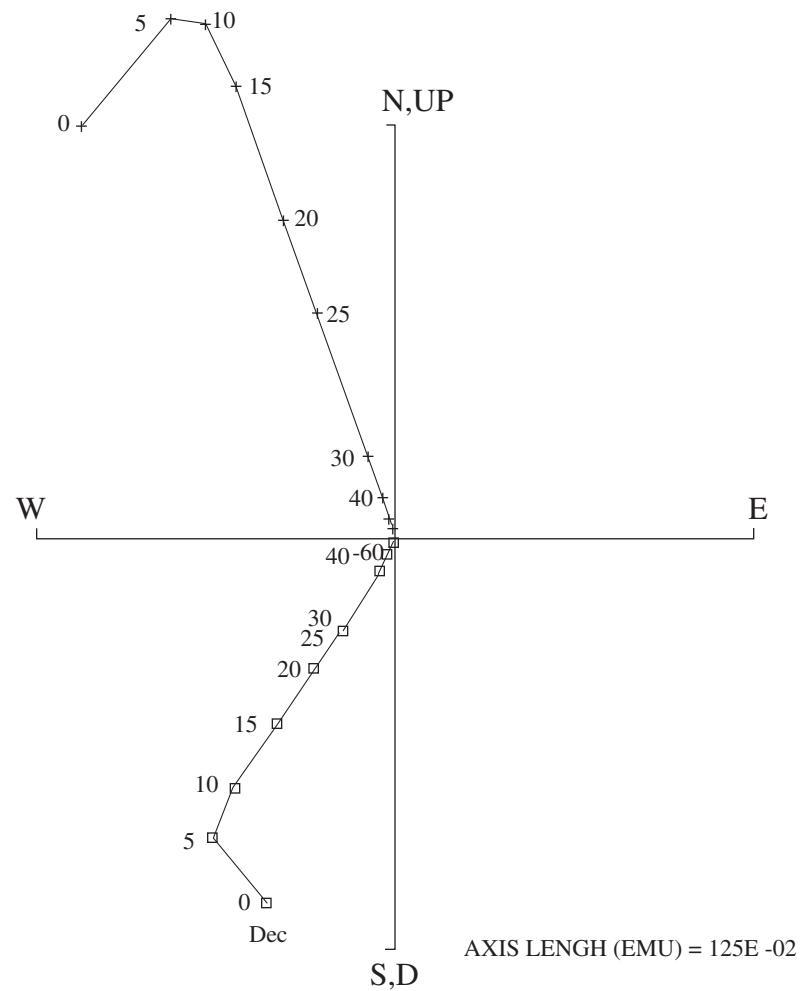
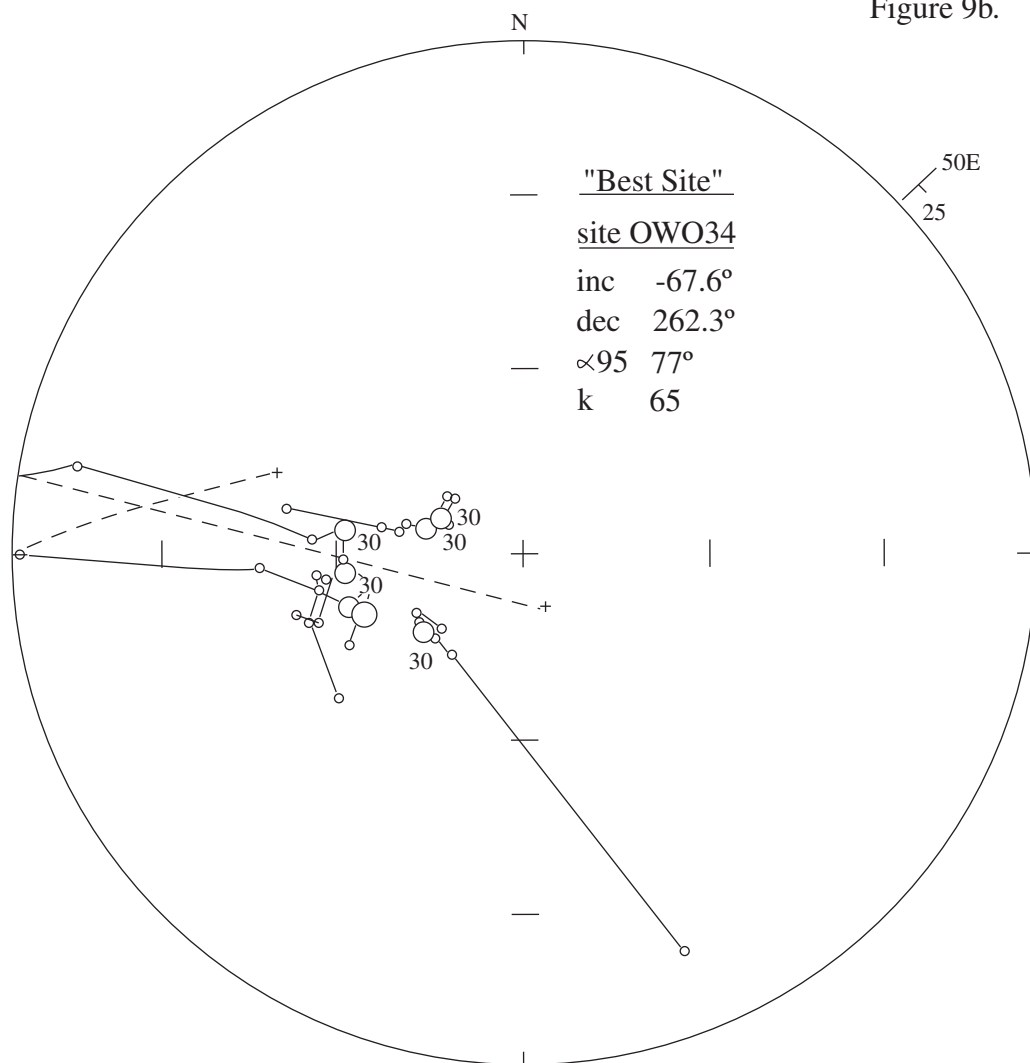
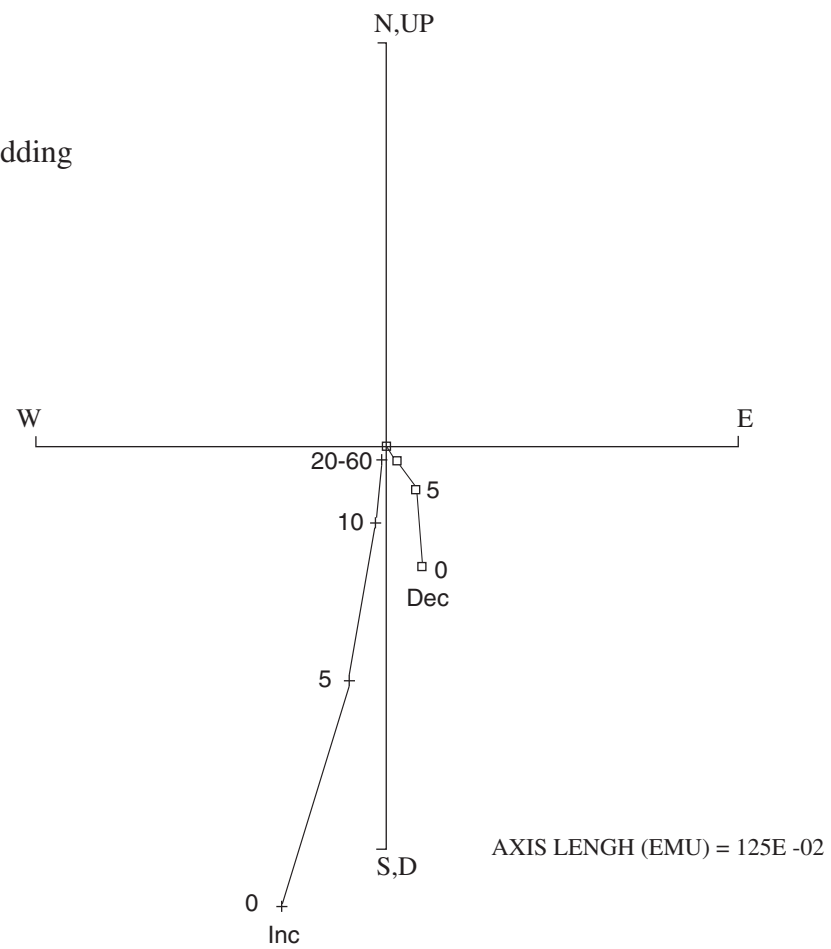
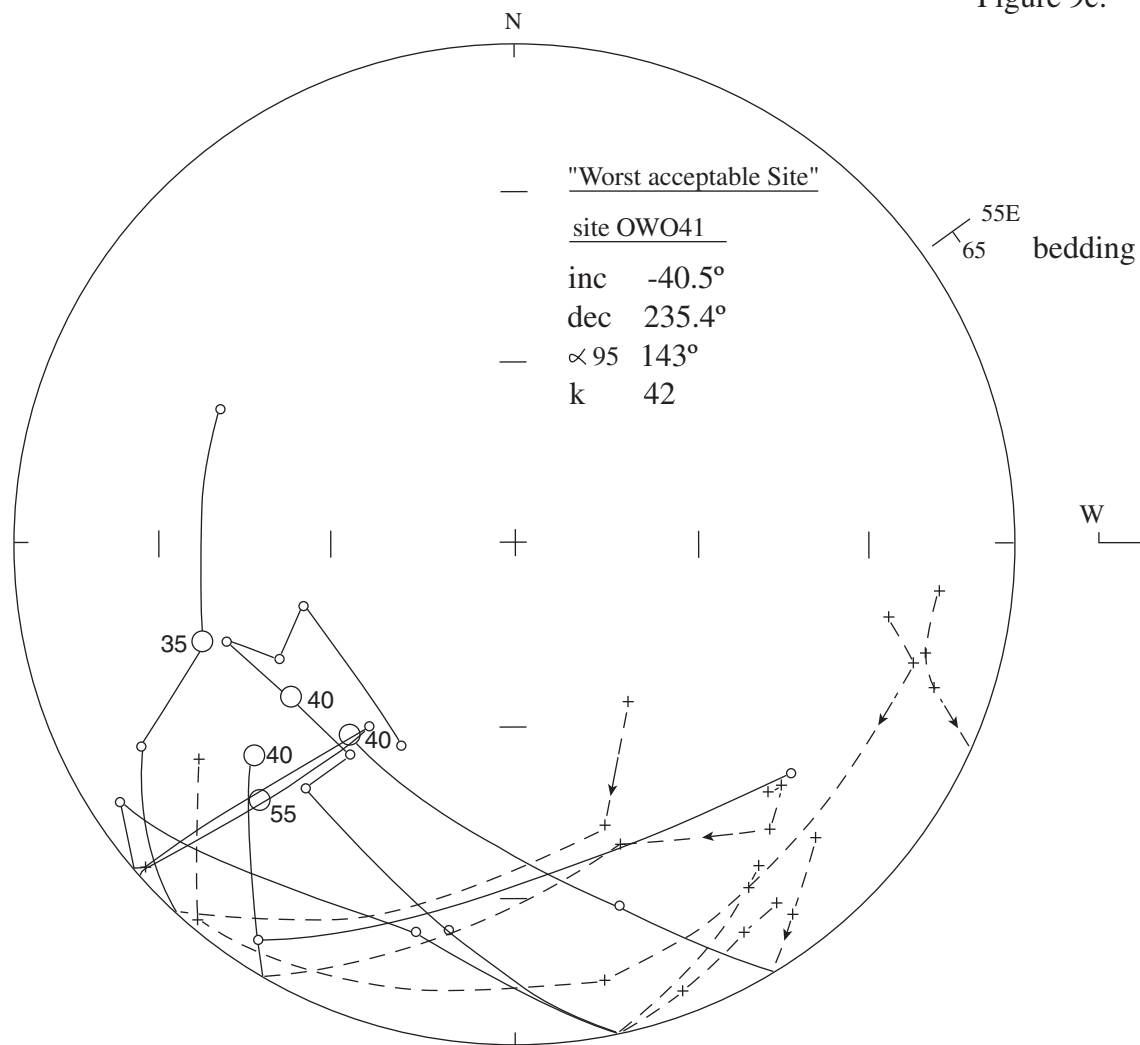


Figure 9c.



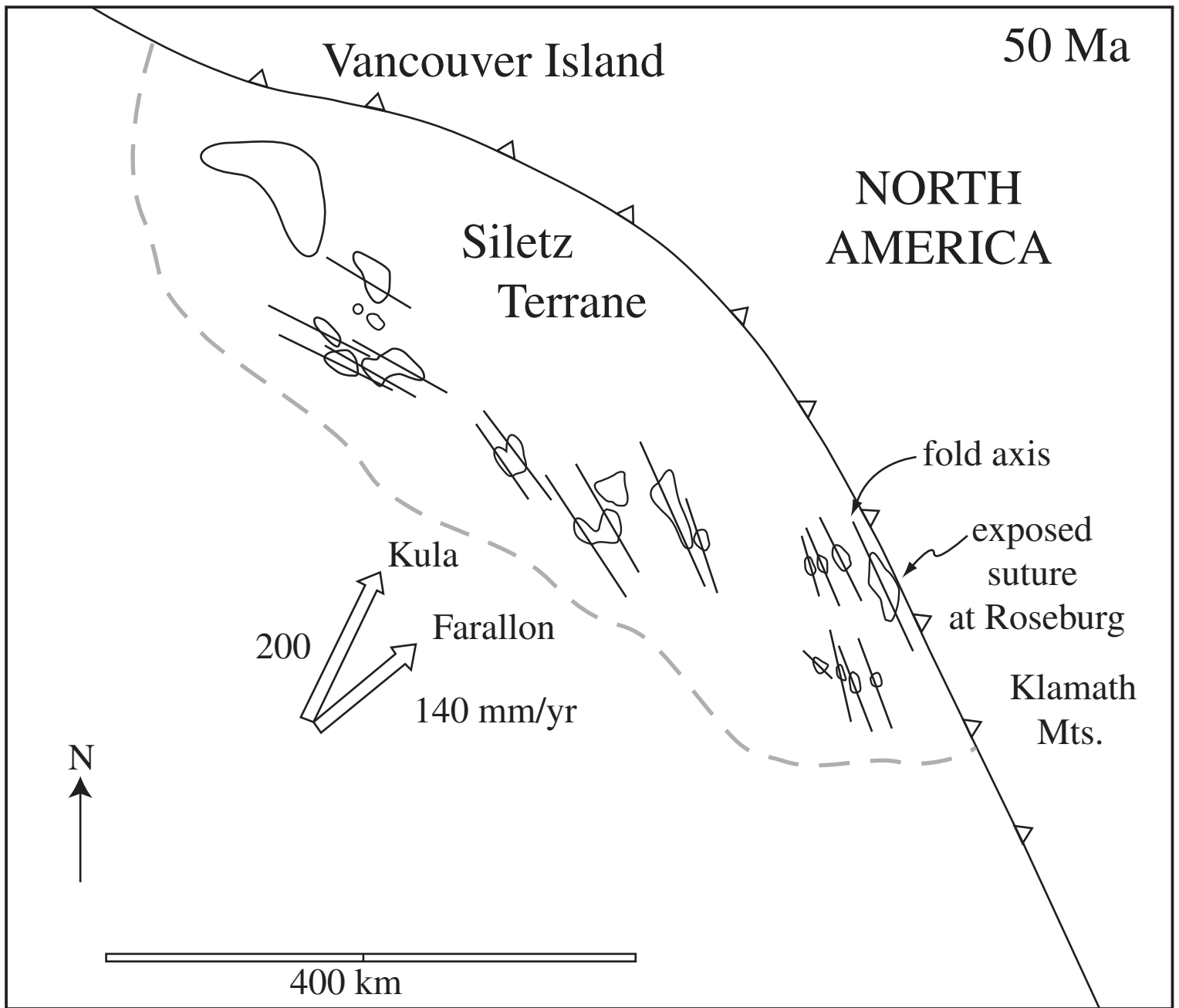


Figure 10. 50 Ma North American margin

Table 1. Oil and gas exploration wells

#	Well Name	Depth	Latitude	Longitude
4	Amoco_Weyerhaeuser_F-1	4,428	43.406	-123.837
5	Amoco_Weyerhaeuser_B-1	11,330	43.386	-123.714
6	Sheldon_C._Clark_"Oakland_well	2,235	43.405	-123.311
7	Mobil_Oil_Corp._Sutherlin_Unit_1	13,177	43.434	-123.238
8	Union_Oil_Co._Liles_1	7,002	43.3617	-123.506
9	Hutchins_&_Marrs_Glory_Hole_1	2,987	43.238	-123.521
10	Community_Oil_&_Gas_Co._Scott_1	3,693	43.242	-123.44
11	Diamond_Drill_Contracting_Co._Hamilton_Ranch_Well_3	545	43.246	-123.511
12	Diamond_Drill_Contracting_Co._Hamilton_Ranch_Well_1	628	43.182	-123.553
13	Diamond_Drill_Contracting_Co._Hamilton_Ranch_Well_2	1,109	43.221	-123.515
14	W._F._Kernin_Well_1	3,900	43.217	-123.417
15	F._W._Dillard_unnamed	700	43.176	-123.474
16	Uranium_Oil_&_Gas_Co._Ziedrich_1	4,368	43.0512	-123.657

well number from Niem and Niem (1990)

Table 2a) Paleontology Database Cocoliths and Forams

<u>Record Number</u>	<u>Sample Number</u>	<u>Unit</u>	<u>Location</u>	<u>Qtr.</u>	<u>S</u>	<u>T</u>	<u>R</u>	<u>Formainifera</u>	<u>Paleodepth</u>	<u>Cocolith</u>	<u>Longitude</u>	<u>Latitude</u>
				<u>Sect.</u>				<u>Age</u>		<u>Age</u>	<u>West</u>	<u>North</u>
1	RN-91-103	Coquille River	Camas Valley	NE	36	29	9	Indet.	IN-MN		123.70	43.01
2	RN-90-280	Camas Valley	Camas Valley	NW	16	29	8			10 to 12a	123.66	43.05
3	RN-90-287	Hubbard Creek	Bingham Creek	NW	22	29	9	A2-B	ON Deeper		123.75	43.03
4	RN-90-284	Tyee Mountain	Bingham Creek	SE	22	29	9	A1			123.74	43.03
5	RN-90-290	Hubbard Creek	Bingham Creek	NW	22	29	9	B1-A	?		123.76	43.03
6	RN-91-396	Camas Valley	Remote	SE	33	29	10			11	123.88	43.00
7	RN-91-394	Camas Valley	Remote	SE	33	29	10			11	123.88	43.00
8	RN-91-183	Rasler Creek	Remote	SW	34	29	10	B1	Bathyal		123.88	43.00
9	RN-91-178	Camas Valley	Remote	SE	28	29	10			11 to 12a	123.88	43.01
10	RN-91-179	Camas Valley	Remote	SE	28	29	10	B1	LMB	11	123.88	43.01
11	RN-91-180	Camas Valley	Remote	SE	28	29	10			11	123.88	43.01
12	RN-91-162	Berry Creek	Remote	NE	30	29	10	B4	UB	11	123.92	43.02
13	RN-91-245	Tenmile	Remote	NW	30	29	10	Paleogene	ON Deeper		123.93	43.02
14	RN-91-251	Tenmile	Remote	NW	30	29	10			10 to 11	123.93	43.02
15	RN-91-252	Tenmile	Remote	NW	30	29	10	B4	Neritic	10 to 11	123.92	43.02
16	RN-91-268	Berry Creek	Rasler Creek	SW	23	29	11	B Older	Neritic	11	123.98	43.04
17	N-90-256A	Coquille River	Dora	NE	8	28	10	B1A(7 Older)	UB		123.90	43.15
18	N-90-256B	Coquille River	Dora	NE	8	28	10	B1A	ON		123.90	43.15
19	N-90-243	Berry Creek	Dora	SE	6	28	10	B4	UB		123.92	43.16
20	F1-4100	Umpqua Undiff.	Ivers Peak	NE	11	25	10	B4-C	Neritic	11	123.86	43.41
21	F1-3600	Umpqua Undiff.	Ivers Peak	NE	11	25	10	B4-C	LMB	11	123.86	43.41
22	F1-3500	Umpqua Undiff.	Ivers Peak	NE	11	25	10	B4-C	LMB	11	123.86	43.41
23	B1-6990	Umpqua Undiff.	Williams Ck.	NE	24	25	9	C	Bathyal	11	123.71	43.40
24	B1-6970	Umpqua Undiff.	Williams Ck.	NE	24	25	9	C	Bathyal	11	123.71	43.40
25	B1-6900	Umpqua Undiff.	Williams Ck.	NE	24	25	9	B4	Bathyal	11	123.71	43.40
26	B1-4900	Tyee Mountain	Williams Ck.	NE	24	25	9	Indet.	Indet.	Eocene	123.71	43.40
27	B1-3610	Tyee Mountain	Williams Ck.	NE	24	25	9	Indet.	Marine	10 to 14	123.71	43.40
28	B1-2920	Tyee Mountain	Williams Ck.	NE	24	25	9	Indet.	Indet.	Eocene	123.71	43.40
29	B1-1420	Elkton	Williams Ck.	NE	24	25	9	A2-B	ON-UB	Eocene	123.71	43.40

30	B1-1240	Elkton	Williams Ck.	NE	24	25	9	A2-B	ON-UB	E. Eocene	123.71	43.40
31	R-89-163	Bateman	Radar Creek	NW	9	24	8	A1	Marine		123.66	43.50
32	R-89-166	Bateman	Radar Creek	SW	4	24	8	A1	Bathyal		123.66	43.51
33	R-89-162	Bateman	Radar Creek	Ctr.	9	24	8	A2	Marine		123.65	43.50
34	RN-91-126	Tyee Mountain	Callahan Road	NW	4	27	7	A2-B	Marine		123.54	43.25
35	R-89-057	Camas Valley	Callahan Road	Ctr.	4	27	7	A2-B	UB-MB	11	123.54	43.25
36	N-90-410	Berry Creek	Glide	NW	19	26	7				123.58	43.30
37	Scott-410	Tenmile	Melrose	SE	8	27	6	C Older (9)	MB	10	123.43	43.25
38	Scott-200	Tenmile	Melrose	SE	8	27	6	C	MB	10	123.43	43.25
39	Scott-100	Tenmile	Melrose	SE	8	27	6	C	LMB	10	123.43	43.25
40	Scott-30	Tenmile	Melrose	SE	8	27	6	C	LMB	10	123.43	43.25
41	N-90-245	Umpqua Undiff.	Coyote Hill	NE	32	26	6	C Older	ON Deeper		123.43	43.27
42	N-90-409	Berry Creek	Glide	NW	19	26	6				123.46	43.30
43	RN-90-010	Umpqua Undiff.	Tyee road	NE	25	25	7			11	123.47	43.37
44	N-90-278	Umpqua Undiff.	Tyee Road	NE	25	25	7			11	123.47	43.37
45	N-90-270	Umpqua Undiff.	Tyee Road	NE	25	25	7	A2-B	MB		123.47	43.37
46	N-90-269	Umpqua Undiff.	Tyee Road	NE	25	25	7	B4 Older	MB	11	123.47	43.37
47	UL-6100	Umpqua Undiff.	Tyee Road	SE	27	25	7	C	Marine	10 to 11	123.51	43.37
48	UL-4800	Umpqua Undiff.	Tyee Road	SE	27	25	7	C	Neritic	10 to 11	123.51	43.37
49	UL-3900	Umpqua Undiff.	Tyee Road	SE	27	25	7	C	Marine	10 to 11	123.51	43.37
50	UL-1900	Umpqua Undiff.	Tyee Road	SE	27	25	7	C	Marine	10	123.51	43.37
51	UL-1300	Umpqua Undiff.	Tyee Road	SE	27	25	7	C	Marine	10 to 11	123.51	43.37
52	UL-1100	Umpqua Undiff.	Tyee Road	SE	27	25	7	C	UMB	10	123.51	43.37
53	UL-820	Umpqua Undiff.	Tyee Road	SE	27	25	7	B4	LMB	10 to 11	123.51	43.37
54	UL-520	Umpqua Undiff.	Tyee Road	SE	27	25	7	B4	LMB	11 to 12a	123.51	43.37
55	UL-240	Umpqua Undiff.	Tyee Road	SE	27	25	7	B4	LMB	11 to 12a	123.51	43.37
56	RN-90-011	Tyee Mountain	Tyee Road	SW	22	25	7			Cenozoic	123.51	43.38
57	R-90-039	Tyee Mountain	Tyee Road	NE	21	25	7	A2-B (4)	UB	10 to 12a	123.53	43.39
58	RN-90-012	Tyee Mountain	Tyee Road	NW	22	25	7			M. Eocene	123.52	43.38
59	R-90-045	Tyee Mountain	Tyee Road	SW	10	25	7			10 to 12a	123.52	43.41
60	R-90-046	Tyee Mountain	Tyee Road	SW	9	25	7			M. Eocene	123.54	43.41
61	RN-90-029A	Hubbard Creek	Tyee Road	SE	8	25	7			12b ?	123.55	43.41
62	RN-90-029B	Hubbard Creek	Tyee Road	Ctr.	8	25	7			12b ?	123.56	43.41

63	N-90-284	Tyee Mountain	Tyee Road	SW	23	25	7	B1A	ON-UB		123.50	43.38
64	N-90-408	Berry Creek	Glide	NW	19	26	5				123.34	43.30
65	R-89-159	Umpqua Undiff.	Sutherlin Creek	SW	19	25	5	A2 Older	Marine		123.34	43.38
66	RN-91-141	Umpqua Undiff.	Calapooya Ck.	Ctr.	1	25	5	A2 OLDER	Marine		123.24	43.42
67	RN-91-139	Umpqua Undiff.	Calapooya Ck.	Ctr.	1	25	5	A2 OLDER	Marine		123.24	43.42
68	RN-91-138	Umpqua Undiff.	Calapooya Ck.	Ctr.	1	25	5	A2 OLDER	Bathyal	10 to 12a	123.24	43.42
69	RN-91-137	Umpqua Undiff.	Calapooya Ck.	Ctr.	1	25	5	B	Open Marine	10 to 12a	123.24	43.42
70	RN-91-132	Umpqua Undiff.	Calapooya Ck.	Ctr.	1	25	5	A2 Older	Bathyal		123.24	43.43
71	MS-3990	Umpqua Undiff.	Calapooya Ck.	SW	36	24	5	C	LMB	10	123.24	43.44
72	MS-3900	Umpqua Undiff.	Calapooya Ck.	SW	36	24	5	C	LMB	Barren	123.24	43.44
73	MS-3800	Umpqua Undiff.	Calapooya Ck.	SW	36	24	5	C	LMB	10	123.24	43.44
74	MS-1200	Umpqua Undiff.	Calapooya Ck.	SW	36	24	5	B	Marine	10 to 11	123.24	43.44
75	MS-800	Umpqua Undiff.	Calapooya Ck.	SW	36	24	5	b	Marine	10	123.24	43.44
76	MS-600	Umpqua Undiff.	Calapooya Ck.	SW	36	24	5	B	ON deeper	Barren	123.24	43.44
77	RN-91-144	Umpqua Undiff.	Metz Hill (T)	Ctr.	32	24	5	B Older	ON-UB		123.31	43.44
78	RN-91-146	Umpqua Undiff.	Metz Hill (T)	Ctr.	32	24	5	B Older (7)	IN-MN	Eocene	123.31	43.44
79	RN-91-145	Umpqua Undiff.	Metz Hill (T)	Ctr.	32	24	5	A2 Older	Bathyal		123.31	43.44
80	RN-91-147	Umpqua Undiff.	Metz Hill (T)	Ctr.	32	24	5	B (7)	UB	11	123.31	43.44
81	RN-91-148	Umpqua Undiff.	Metz Hill (T)	Ctr.	32	24	5	B	UB	11	123.31	43.44
82	RN-91-149	Umpqua Undiff.	Metz Hill (T)	Ctr.	32	24	5	B (6)	MB	11	123.31	43.44
83	RN-91-151	Umpqua Undiff.	Metz Hill (T)	Ctr.	32	24	5	A2-B	UB	10 to 12a	123.31	43.44
84	N-91-133	Umpqua Undiff.	Metz Hill	NW	32	24	5	A2-B	ON Deeper	10 to 11	123.32	43.45
85	N-91-137	Umpqua Undiff.	Metz Hill	NW	32	24	5	A2-B	ON Deeper	10 to 11	123.32	43.45
86	N-91-138	Umpqua Undiff.	Metz Hill	NW	32	24	5	A2-B	ON Deeper		123.32	43.44
87	N-91-140	Umpqua Undiff.	Metz Hill	NW	32	24	5	A2 Older	Marine Undiff.		123.32	43.44
88	RN-91-028	Bushnell	Glide	NE	16	26	4	A2-B?	ON-UB		123.17	43.31
89	N-91-053	Umpqua Undiff.	Glide	NE	16	26	4	D	Marine Undiff.		123.17	43.32
90	RN-91-029	Tenmile	Glide	Ctr.	14	26	4	A2-B?	ON-UB		123.14	43.31
91	RN-91-030	Tenmile	Glide	Ctr.	14	26	4	A2-B?	ON-UB	Barren	123.14	43.31
92	RN-91-032	Tenmile	Glide	Ctr.	14	26	4	A2 Older	Marine		123.14	43.31
93	RN-91-031	Tenmile	Glide	Ctr.	14	26	4	A2-B?	UB		123.14	43.31
94	RN-91-036	Tenmile	Glide	Ctr.	14	26	4	A2 Older	Marine		123.13	43.31
95	N-90-250	Berry Creek	Glide	NW	19	26	3	B4	MB		123.11	43.30

96	N-90-295	Berry Creek	Glide	NW	19	26	3					123.10	43.30
97	N-90-415	Berry Creek	Glide	NW	19	26	3	B	Neritic			123.10	43.30
98	N-90-386	Coquille River	Glide	W	17	26	3	A2	U-MB	11		123.08	43.30
99	N-90-391	Camas Valley	Glide	N	17	26	3	B1	ON Deeper			123.09	43.31
100	N-90-390	Camas Valley	Glide	N	17	26	3	B1	ON Deeper	M. Eocene		123.09	43.31
101	N-90-389	Camas Valley	Glide	N	17	26	3	B1	ON Deeper	11		123.09	43.31
102	N-90-370	Camas Valley	Glide	N	17	26	3	B1	ON Deeper			123.09	43.31
103	N-90-369	Camas Valley	Glide	N	17	26	3	B1	ON Deeper	11		123.08	43.31
104	N-90-361	Camas Valley	Glide	N	17	26	3	B1	Neritic			123.07	43.31
105	N-90-363	Camas Valley	Glide	N	17	26	3	B1	Neritic			123.07	43.31
106	N-90-364	Camas Valley	Glide	N	17	26	3	B1	ON			123.08	43.31
107	N-90-367	Camas Valley	Glide	N	17	26	3	B1	UB	11		123.08	43.31
108	N-90-366	Camas Valley	Glide	N	17	26	3	B1A	UB			123.08	43.31
109	N-90-287	Camas Valley	Camas Valley	NW	16	29	8	B1 (5)	MB	Eocene		123.66	43.05
110	N-90-288	Camas Valley	Camas Valley	NW	16	29	8	B1 (5)	MB			123.66	43.05
111	UZ-4132	Tenmile	Camas Valley	NW	16	29	8			10		123.66	43.05
112	UZ-3618	Tenmile	Camas Valley	NW	16	29	8			10		123.66	43.05
113	UZ-3272	Tenmile	Camas Valley	NW	16	29	8			10		123.66	43.05
114	R-89-105	Tenmile	Suicide Creek	SE	2	29	8	C Older	Marine Undiff.			123.61	43.07
115	R-89-104	Tenmile	Suicide Creek	SE	2	29	8	C Older	Marine Undiff.			123.60	43.07
116	R-89-124	Tenmile	Suicide Creek	SE	3	29	8	C Older	LMB	Eocene		123.62	43.07
117	R-89-114	Tenmile	Suicide Creek	SE	3	29	8	C Older	Indet.			123.63	43.07
118	R-89-110	Tenmile	Suicide Creek	Ctr.	3	29	8	C Older	Marine			123.63	43.08
119	R-89-108	Tenmile	Suicide Creek	Ctr.	3	29	8	C Older	Marine			123.63	43.08
120	R-89-107	Tenmile	Suicide Creek	NE	3	29	8	C Older	Marine			123.63	43.08
121	R-89-106	Tenmile	Suicide Creek	SE	34	28	8			Eocene		123.63	43.08
122	R-89-099	Tenmile	Suicide Creek	NE	2	29	8	C Older	Marine Undiff.			123.61	43.08
123	R-89-088	Tenmile	Suicide Creek	SW	35	28	8	C Older (9)	Bathyal			123.61	43.08
124	R-89-086	Tenmile	Suicide Creek	SW	35	28	8	C Older	ON			123.62	43.09
125	R-89-084	Tenmile	Suicide Creek	NE	34	28	8	C Older	Marine			123.62	43.09
126	N-90-225	Umpqua Undiff.	Reston Road Reston	NE	25	28	8	C	Marine Undiff.			123.59	43.11
127	R-89-127	Tenmile	Junction	SW	14	28	8	C Older	UB Deeper			123.62	43.13
128	R-89-075	Umpqua Undiff.	Reston Road	SW	14	28	8	C Older	Marine			123.62	43.13

129	R-89-073	Umpqua Undiff.	Reston Road	SW	14	28	8	C Older	ON-UB		123.62	43.13
130	N-90-222	Tenmile	Reston Junction	SE	11	28	8	A2 Older	MB		123.61	43.14
131	RN-91-123	Tenmile	Reston Junction	SE	11	28	8	B	MB	11	123.61	43.14
132	N-91-130A	Tenmile	Burnt Ridge	N	16	28	8	Cretaceous ?	ON Deeper	10 Older	123.65	43.14
133	RN-91-125	Camas Valley	Burnt Ridge	Ctr.	9	28	8	A2-B	Marine		123.65	43.15
134	RN-91-109	Hubbard Creek	Burnt Ridge	Ctr.	4	28	8	A2-B	Open Marine	M. Eocene	123.65	43.16
135	R-89-072	Umpqua Undiff.	Reston Road	NE	25	28	8	C Older(9)	UMB	10	123.59	43.11
137	RN-91-118	Coquille River	Callahan Road	SE	4	27	7	B1	Bathyal		123.53	43.24
138	GH-2910	Tenmile	Melrose	NE	10	27	7	Indet.	Marine Undiff.	Cenozoic	123.51	43.24
139	GH-1670	Tenmile	Melrose	NE	10	27	7	Indet.	Marine Undiff.	Cenozoic	123.51	43.24
140	GH-1020	Berry Creek	Melrose	NE	10	27	7	Indet.	Marine Undiff.	Nondiag.	123.51	43.24
141	GH-690	Berry Creek	Melrose	NE	10	27	7	B	Neritic	Nondiag.	123.51	43.24
142	N-91-117	Berry Creek	Melrose	SW	5	27	6	Indet.	Tidal Flat		123.44	43.25
143	RN-91-231	Tyee Mountain	F-1	NW	10	25	10	B1?	Bathyal		123.87	43.42
144	RN-91-295	Tyee Mountain	F-1	NW	10	25	10			M. Eocene	123.87	43.41
145	RN-91-296	Tyee Mountain	F-1	NW	10	25	10	B		Cenozoic	123.87	43.41
146	RN-91-208B	Tenmile	LaVern Creek	NW	5	27	11	B4-C	LMB	10	124.02	43.26
147	RN-91-207	Tenmile	LaVern Creek	NW	5	27	11	B4-C	LMN		124.02	43.26
148	RN-91-204	Tenmile	LaVern Creek	NW	5	27	11			11	124.02	43.26
149	RN-91-221	Hubbard Creek	Middle Creek	NE	1	27	11	A2-B1	LMB		123.96	43.26
150	RN-91-223A	Hubbard Creek	Middle Creek	NE	1	27	11			12a	123.96	43.26
151	RN-91-220	Tyee Mountain	Middle Creek	NW	6	27	10			12a	123.94	43.25
152	N-90-220	Camas Valley	Wagon Road	SW	6	28	10	B1	UB		123.94	43.16
153	N-90-220B	Camas Valley	Wagon Road	SW	6	28	10	B1	UB		123.94	43.16
154	N-90-220C	Camas Valley	Wagon Road	SW	6	28	10	B1	UB		123.94	43.16
155	RN-91-255	Hubbard Creek	Sandy Creek	SE	22	28	10	A2	Bathyal		123.86	43.11
156	RN-90-274	Tyee Mountain	Lost lake	SE	25	28	9			10 to 14	123.71	43.10
157	W-90-22B	Bushnell Rock	Look Glass ck.	SE	39	28	7			Paleocene	123.47	43.14
158	W90-8b	Tmms		NE	25	27	6				123.35	43.19
160	W93-43b	Slater Creek	Calapoova Crk.	SW	10	25	4			CP10 to 12a	123.35	43.25
161	W94-35a	Tsrs	S.Umpqua R.	NE	2	28	6			Paleocene	123.37	43.17
162	W94-39d	Tsrs	look glass crk	SW	16	28	7			Paleocene	123.50	43.14
163	W94-52b	Tsrs		NE	41	27	5			Paleocene	123.28	43.22

164	W94-5a	Tmm	runway	NW	19	24	5			CP11	123.34	43.48
165	W94-5b	Tmm	runway	NW	19	24	5			CP11	123.34	43.48
166	W95-27	Elkton Fm	Arrow crk	NE	33	25	8			Eocene	123.68	43.36
167	W95-6	Bateman Fm		cen	2	26	8			Eocene	123.62	43.34
168	W95-8	Tyee Fm	Cedar crk	SW	6	26	8			Eocene	123.69	43.33
169	W95-9d	Bushnell	Roseburg	NE	61	27	6			CP10 to12a	123.35	43.25
170	W96-4d	Tmms	Umpqua R	NW	8	26	6			CP10/12	123.44	43.33
171	W96-7d	Tmms	Suth crk.	SE	31	25	5			CP10-late	123.33	43.35
172	S80-10	Tmm	Bachelor crk	NW	19	24	4			CP11	123.22	43.47
173	W-96-10a-d	Tmms	Umpqua R.	SW	5	26	6			CP10/12	123.44	43.33
174	W95-9b	Bushnell	Roseburg	NE	61	27	6			CP10	123.35	43.25
175	W92-15	Busnell Rock	Oak creek	CEN	31	25	4			Mid-Eocene	123.22	43.35
176	N-91-021	Tenmile	Glide	Ctr.	40	26	4	A2 Older	Marine Undiff.		123.14	43.30
177	N-91-022	Tenmile	Glide	Ctr.	40	26	4	10	Neritic	10	123.14	43.30
178	N-91-023	Tenmile	Glide	Ctr.	40	26	4	D	U-MB	10 Older	123.14	43.30
179	N-91-025	Tenmile	Glide	Ctr.	40	26	4	C Older	ON Deeper		123.14	43.30
180	N-91-016	Tenmile	Glide	Ctr.	40	26	4			E. Eocene	123.14	43.30
181	N-91-012	Tenmile	Glide	W	40	26	4	A2 Older	Marine undiff		123.14	43.30
182	N-91-011	Tenmile	Glide	W	40	26	4	C	M-ON	10	123.14	43.30
183	N-91-009	Tenmile	Glide	Ctr.	40	26	4	C	ON-UB	10	123.14	43.30
184	N-91-041	Tenmile	Glide	NW	39	26	4	B Older	ON UB		123.12	43.30
185	N-91-036	Tenmile	Glide	Ctr.	39	26	4	C Older	UB	10	123.12	43.30
186	N-90-304	Tenmile	Glide	Ctr.	39	26	4	C	UB	10	123.12	43.30
187	N-91-131	Umpqua Undiff.	Metz Hill	Ctr.	38	24	5	A2-B	U-MB	10	123.32	43.46
188	N-91-131A	Umpqua Undiff.	Metz Hill	Ctr.	38	24	5	A2-B	U-MB		123.32	43.46
189	N-91-132	Umpqua Undiff.	Metz Hill	Ctr.	38	24	5	A2-B	ON Deeper	10 to 11	123.32	43.46
190	W96-8a-c	Tmms		SE	31	25	5			CP10-Late	123.33	43.35
191	W90-10	Kjda		NE	13	28	6			E. Cretaceous	123.35	43.14

Key Foraminifera Paleodepth

Bathyal	Bathyal	Marine Undiff.	Marine Undifferentiated	ON	outter Neritic	UB	upper Bathyal
Indet.	indeterminate	Marine	Marine	ON deeper	otter Neritic Deeper	U-MB	upper-mid. Bathyal
IN-MN	Inner-Neritic to mid. Neritic	MB	Middle Bathyal	Open Marine	Open Marine		
LMB	Lower-Mid. Bathyal	M-ON	Mid.-outter Neritic	ON-UB	outter Neritic-Upper Bathyal		
LMN	Lower-Mid. Neritic	Neritic	Neritic	Tidal Flat	Tidal Flat		

Table 2b) Paleontology Database
Macrofossils

<u>Rec. #</u>	<u>Sample#</u>	<u>Unit.</u>	<u>Location</u>	<u>Age</u>	<u>Paleodepth</u>	<u>1/8th</u>	<u>Qtr.</u>	<u>Section</u>	<u>Township</u>	<u>Range</u>	<u>Longitude</u>	<u>Latitude</u>
						<u>Sec.</u>	<u>Sec.</u>				<u>West</u>	<u>North</u>
1	92LM1	Slater Creek Mbr.	Freer Bridge	e. Paleocen to l. Eocene	20 to 185	NE	NW	43	26s	4w	123.12	43.31
2	92LM2	Sclater cr. Mbr.	Freer Bridge	e. Eocene to l. mid. Eocene	25 to 35	NE	NW	43	26s	4w	123.12	43.31
3	92LM3	Lower TenMile	100ft. E.Freer Bridge	Eocene (maybe e. Eocene)	20 to 185	NE	NW	43	26s	4w	123.12	43.31
4	92LM4	Culvert locality	Camas Valley Fm.	Paleocene to Eocene	10 to 25	SW	NE	17	26s	3w	123.08	43.31
5	92LM5	lower 1/3 TenMile	Gravel Bar	Eocene (maybe e. Eocene)	0 to 150 meters	NE	SW	18	26s	3w	123.10	43.30
6	92LM6	Sclater Cr. Mbr.	Sears-Roseburg,Or		inner to mid. Shelf	Ctr.	Ctr.	11	27s	6w	123.37	43.23
7	92LM7	Sclater Cr. Mbr.	Sears-Roseburg ~ 30ft. Down sec.			Ctr.	Ctr.	11	27s	6w	123.37	43.23
8	92LM8	White Tail Mbr.	Hiwy. 42 Camas Mtn.St. Park	e. mid. Eocene to l. Eocene	~75	SE	NW	9	29s	8w	123.65	43.06
9	92LM9	White Tail Mbr.	same as 92LM8 mid sec	e. mid. Eocene to l. Eocene	50 to 90	SE	NW	9	29s	8w	123.65	43.06
10	92LM10	White Tail Mbr.	county road #36	l. e. Eocene to e. mid. Eocene	~<50	SE	SE	17	27s	4w	123.19	43.22
11	24DV92	White Tail Mbr.	Dixonville 7.5"	e. Eocene to l. mid. Eocene	v. shallow n. shelf	NW	SW	43	27s	4w	123.18	43.21
12	25DV92	White Tail Mbr.	Dixonville 7.5"		Intertidal-shallow	SW	NW	43	27s	4w	123.18	43.22
13	27DV92	Ten Mile	Dixonville 7.5"		20 to 185	NE	NW	16	27s	4w	123.17	43.23
14	28DV92	Slater Creek Mbr.	Dixonville 7.5"		n. shoreline	SW	SE	9	27s	4w	123.18	43.23
15	29DV92	Slater Creek Mbr.	Dixonville 7.5"			SE	NE	9	27s	4w	123.17	43.24
16	31DV92	Ten Mile	Dixonville 7.5"		20 to 180	NW	SE	41	27s	4w	123.16	43.25
17	1LM92	White Tail Ridge	Lane Mountain 7.5"	Paleocene to early Oligocene	~<50	NE	NW	8	27s	3w	123.08	43.24
18	2LM92	White Tail Ridge	Lane Mountain 7.5"			SE	NW	8	27s	3w	123.08	43.24
19	3LM92	White Tail Ridge	Lane Mountain 7.5"			SE	NW	8	27s	3w	123.08	43.24
20	4LM92	White Tail Ridge	Lane Mountain 7.5"			SE	NW	8	27s	3w	123.08	43.24
21	9LM92	White Tail Ridge	Lane Mountain 7.5"	e. Eocene to l. mid. Eocene	20 to 185	NW	SW	7	27s	3w	123.11	43.23
22	10LM92	White Tail Ridge	Lane Mountain 7.5"	Paleocene to l. Eocene	~<50	NW	SW	7	27s	3w	123.10	43.23
23	11LM92	White Tail Ridge	Lane Mountain 7.5"	e. Eocene to l. mid. Eocene	20 to 185	SW	SW	7	27s	3w	123.10	43.23
24	12LM92	White Tail Ridge	Lane Mountain 7.5"		~20 to 185	SE	SW	7	27s	3w	123.10	43.23
25	14LM92	White Tail Ridge	Lane Mountain 7.5"			SW	SE	12	27s	4w	123.11	43.23
26	15LM92	Tw	Lane Mountain 7.5"			NW	NE	18	27s	3w	123.11	43.22
27	16LM92	Tw	Lane Mountain 7.5"	e. Eocene to l. mid. Eocene	20 to 185	Ctr.	NE	18	27s	3w	123.10	43.22
28	W93-13a	Tsrs-Turbidite	SE Corner of Nonpareil Or 7.5"			NE	NE	23	25s	4W	123.13	43.38
29	W93-13b	Tsrs-Turbidite	SE Corner of Nonpareil Or 7.5"			NE	NE	23	25s	4W	123.13	43.38

30	W93-13c	Tsrs-Turbidite	SE Corner of Nonpareil Or 7.5"			NE	NE	23	25s	4W	123.13	43.38
31	W93-13d	Tsrs-Turbidite	SE Corner of Nonpareil Or 7.5"			NE	NE	23	25s	4W	123.13	43.38
32	W93-13e	Tsrs-Turbidite	SE Corner of Nonpareil Or 7.5"			NE	NE	23	25s	4W	123.13	43.38
33	W93-13f	Tsrs-Turbidite	SE Corner of Nonpareil Or 7.5"			NE	NE	23	25s	4W	123.13	43.38
34	W93-13g	Tsrs-Turbidite	SE Corner of Nonpareil Or 7.5"			NE	NE	23	25s	4W	123.13	43.38
35	W93-13h	Tsrs-Turbidite	SE Corner of Nonpareil Or 7.5"			NE	NE	23	25s	4W	123.13	43.38
36	W93-13i	Tsrs-Turbidite	SE Corner of Nonpareil Or 7.5"			NE	NE	23	25s	4W	123.13	43.38
37	W93-13j	Tsrs-Turbidite	SE Corner of Nonpareil Or 7.5"			NE	NE	23	25s	4W	123.13	43.38
38	W93-13k	Tsrs-Turbidite	SE Corner of Nonpareil Or 7.5"		v. shallow deposit	NE	NE	23	25s	4W	123.13	43.38
39	W93-13L	Tsrs-Turbidite	Top of Siletz River Volcanics	l. Paleocene to e. Oligocene	0 to 25	NE	NE	23	25s	4W	123.13	43.38
40	93LM2	Slater Creek Mbr.	Singleton Rd. OakCreek Valley	l. e. Eocene to e. mid. Eocene	<50 possible<25	NE	NW	50	26s	4w	123.15	43.27
41	93LM3	Slater Creek Mbr.	Singleton Rd 40m up sec.from 93LM2	l. e. Eocene to e. mid. Eocene	50 to 100	NW	NE	50	26s	4w	123.15	43.27
42	93LM4	Slater Creek Mbr.	Singleton Rd 50m east of 93LM4			Ctr.	NE	50	26s	4w	123.15	43.27
43	93LM5	Ten Mile Frm?	Oak Cr. Valley 7.5"	l. Paleocene to l. Eocene	20 to 185	NE	NE	50	26s	4w	123.14	43.27
44	93LM6	Tsrs-Turbidite	Kline Rd. off Garden Valley Rd.		dep. n. to shorel	NW	NW	36	26s	6w	123.36	43.27
45	93LM7	Slater Creek Mbr.	Kline Rd. ~ 1.1 mi S. of 93LM	l. Paleocene to l. Eocene	0 to 100	NE	NE	2	27s	6w	123.37	43.26
46	93LM8	Slater Creek Mbr.	Ridge n. Roseburg Airport	l. e. Eocene to l. Eocene	20 to 185	SE	NE	61	27s	6w	123.35	43.25
47	93LM9	Slater Creek Mbr.	Base of hill under powerline E of W		20 to 185	SE	NW	51	26s	5w	123.34	43.28
48	93LM10	Slater Creek Mbr.	Rd.cut W. side of I-5 N of Winch.			SW	NW	53	26s	6w	123.36	43.28
49	93LM11	Whitetail Ridge	Rd.cut off Buckhorn Rd.	Eocene	20 to 185	SW	SW	7	27s	3w	123.10	43.23
50	93LM12	Whitetail Ridge	Rd.cut off Buckhorn Rd.	Eocene	20 to 185	SW	SW	7	27s	3w	123.10	43.23
51	N-90-256A	Coquille River	Dora 7.5"		15 to 35		NE	8	28	10	-123.90	43.15
52	N-90-256B	Coquille River	Dora 7.5"		15 to 35		NE	8	28	10	-123.90	43.15
53	N-90-410	Berry Creek	Glide 7.5"		55 to 65		NW	19	26	7	-123.58	43.30
54	N-90-409	Berry Creek	Glide 7.5"		55 to 65		NW	19	26	6	-123.46	43.30
55	N-90-408	Berry Creek	Glide 7.5"		55 to 65		NW	19	26	5	-123.34	43.30
56	N-90-250	Berry Creek	Glide 7.5"		15 to 35		NW	19	26	3	-123.11	43.30
57	N-90-295	Berry Creek	Glide 7.5"		15 to 35		NW	19	26	3	-123.10	43.30
58	N-90-364	Camas Valley	Glide 7.5"		15 to 35		N	17	26	3	-123.08	43.31
59	N-90-366	Camas Valley	Glide 7.5"		15 to 35		N	17	26	3	-123.08	43.31
60	N-90-389	Camas Valley	Glide 7.5"		15 to 35		N	17	26	3	-123.09	43.31
61	93DB-3	JKr-sandstone	Dodson Butte 7.5"	Berriasian		SW	SE	6	29s	4w	-123.21	43.07
62	3-92-DB	JKr-sandstone	Dodson Butte 7.5"	Berriasian		SW	SE	32	29s	4w	-123.20	43.08
63	7DB-92	JKr-sandstone	Dodson Butte 7.5"	Berriasian		SE	NE	2	28s	5w	-123.25	43.08

64	93DB-4	JKr-sandstone	Dodson Butte 7.5"	Berriasian	NW	SE	6	29s	4w	-123.21	43.08
65	93DB-5	JKr-sandstone	Dodson Butte 7.5"	Berriasian	NE	NW	6	29s	4w	-123.22	43.08
66	8DB-92	JKr-sandstone	Dodson Butte 7.5"	Berriasian	NW	SE	36	28s	5w	-123.24	43.09
67	93WR-13	Days Creek Fm.	White Rock 7.5"	Early- Middle Valanginaian	Ctr.	SE	33	29s	3w	-123.07	43.01
68	93WR-14	Days Creek Fm.	White Rock 7.5"	Jurassic-Cretaceous	Ctr.	SE	33	29s	3w	-123.07	43.01
69	94M-6	JKr-sandstone	Myrtle Creek 7.5"	Berriasian	CEN	NE	46	29s	5w	-123.26	43.02
70	3MC-92	KJrc-cong.	Myrtle Creek 7.5"	Oxfordian-Valanginian	SW	NW	2	29s	5w	-123.26	43.08
71	2MC-92	KJrc-cong.	Myrtle Creek 7.5"	Oxfordian-Valanginian	SW	NW	2	29s	5w	-123.26	43.08
72	94M-14	KJrc-cong.	Myrtle Creek 7.5"	Buchia sp.	cen	cen	35	28s	5w	-123.25	43.09
73	94W-6a	JKr?-sandstone	Winston 7.5"	Valanginian	SE	NE	35	29.5S	7w	-123.49	43.00
74	94W-9	JKr?-sandstone	Winston 7.5"	Oxfordian-Valanginian	SE	NW	25	29s	7w	-123.48	43.02
75	94W-14a	JKr?-sandstone	Winston 7.5"	Berriasian?	NE	SE	13	29s	7w	-123.47	43.05
76	94W-14b	JKr?-sandstone	Winston 7.5"	Oxfordian-Valanginian	NE	SE	13	29s	7w	-123.47	43.05
77	94T-1	Jkda	Tenmile 7.5" - quarry	Tithonian	SW	SW	2	29s	7w	-123.50	43.07

Table

e. = early v. = very

mid. = middle n. = near

l. = late

[illegible]

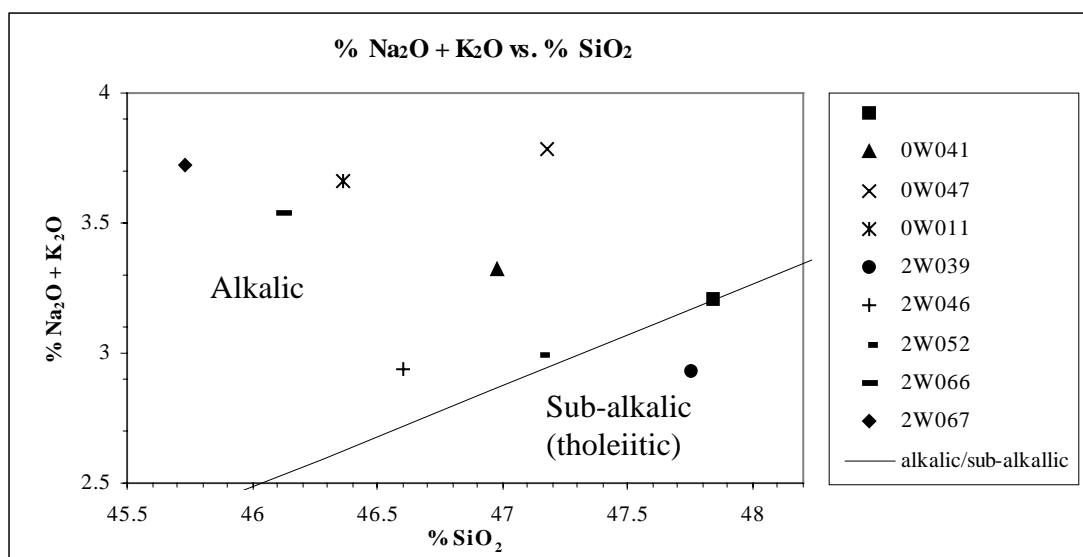
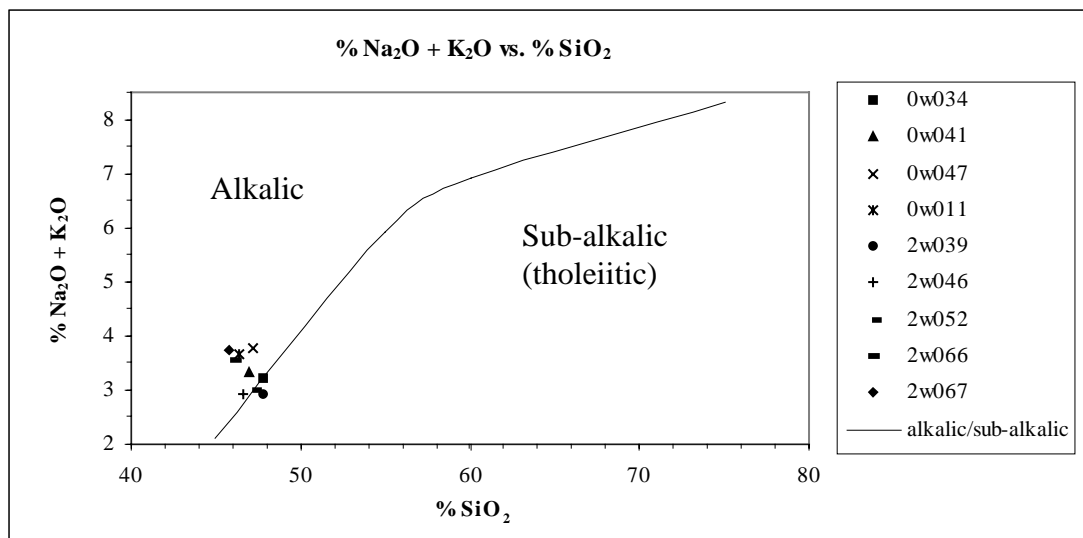
Table 3. Paleomagnetism of the Siletz River Volcanics (SRV) and the Tyee Fore-Arc Basin

Siletz River Volcanics (this paper)										
Site	Location	Lat.	Long.	d/s	Treat.	n/nt	k	alpha95	Ic	Dc
0W034	W side I-5, exit 121	43.181	236.631	25/050	30	7/7	65.4	7.5	-67.6	262.3
0W041	E I-5, Greens District, exit 120	43.165	236.638	64/055	30	4/7	42.2	14.3	-40.5	235.4
0W047	E I-5, Greens District, exit 120	43.165	236.638	64/055	30	5/7	46.7	11.3	-59.1	211.4
2W011	N side Hwy 138, mile E of jct 99	43.215	236.693	17/235	30	6/7	32.5	11.9	-67.6	266.9
2W039	Unnamed quarry, N side Hwy 138	43.222	236.730	38/040	40	7/7	24.8	12.4	-42.9	226.5
2W046	Unnamed quarry, N side Hwy 138	43.222	236.730	62/045	30	4/7	30.2	17.0	-41.9	255.0
2W052	Unnamed quarry, N side Hwy 138	43.22	236.730	38/025	40	7/7	22.9	12.9	-32.9	244.2
2W066	Quarry/road cuts,I-5, Turkey Hill	43.49	236.672	22/065	40	7/7	62.0	7.7	-46.0	261.9
2W076	Quarry/road cuts,I-5, Turkey Hill	43.49	236.672	16/220	60	8/8	17.2	13.7	-26.8	256.5
OSU 1	E of Roseburg, N Side of Hwy 42	43.13	235.86	22/157	20	4/6	69.5	11.1	-72.2	259.7
OSU 2	E of Roseburg, N Side of Hwy 42	43.13	235.86	34/037	20	6/6	30.8	12.3	-78.0	313.0
OSU 4	9 mi E of Roseburg, Lookingglass	43.33	236.793	46/103	25	5/5	17.5	18.8	-48.6	267.5
OSU 5	7 mi W of Glide, N of Umpqua R.	43.33	236.793	41/314	25	6/6	21.4	14.8	-33.1	222.5
OSU 6	7 mi W of Glide, N of Umpqua R.	44.33	236.793	30/023	25	7/7	44.5	9.2	-55.0	232.0
		Lat.		Long.	n/nt	k	alpha95	Inc	Dec	
	Tilt corrected	12	17.9	10.5	-46.9	245.9	
	Tilt uncorrected	12	6.4	18.6	-46.8	220.6	
	Avg site locality	43.25		236.75	
	SRV Formation Direction	14	15.9	10.3	-52.5	246.3	
	SRV Formation Pole	39.00		130.50	14	11.3	12.4	
	N. Am. Reference Pole	81.50		167.40	3.2	
	Latitude Shift at Site	9.57 +/- 9.99		
	Rotation of Site	78.90 +/- 12.53		
Tyee Fore-Arc Basin (Simpson,1977)										
Site		Lat.	Long.	d/s	Treat	n/nt	alpha95	Ic	Dc	
201		43.033	123.865	15/337	10	4/4	23.5	50	13.9	
351		43.449	123.538	10/160	30	6/6	14.4	70.1	65.3	
352		43.449	123.538	10/160	20	5/5	17.1	74.5	132.2	
361		43.137	123.64	70/62.5	20	8/8	16.1	55.7	101.4	
1472		43.414	124.052	11.5/77	15	9/10	4.5	54.7	47.9	
1473		43.414	124.052	11.5/77	20	8/8	4.2	59.8	51.7	
1481		43.414	124.052	9.5/95	15	9/9	7.5	69.3	95.0	
1491		43.442	124.001	6.5/226	15	10/10	9.7	65.3	87.0	
1571		43.387	123.533	10/221	28	8/11	20.8	-46.2	231.9	
1581		43.444	123.602	9.5/128.5	20	8/8	6.9	66.3	72.7	
1582		43.444	123.602	9.5/128.5	15	7/7	10.7	51.8	77.4	
1583		43.444	123.602	9.5/128.6	15	9/9	30.9	45.1	75.4	
1591		43.483	123.613	2/90	15	8/8	6.5	67.7	22.7	
1611		43.532	123.642	10/218	15	7/10	8.6	69.6	50.4	

"Lat.," "Long.," "d/s," "alpha95," "Ic," "Dc" are latitude, longitude, dip and strike (left-hand azimuth looking down dip), radius of alpha 95 cone of confidence, inclination and declination corrected for tilt of flows, all in degrees. "Treat" is alternating field in nanoTeslas that produces best grouping of directions, "n/nt" is number of cores used for mean over total cores collected, "k" is the precision parameter of Fisher (1953). OSU site 1 through 6 from Schultz and McElwee (unpublished ms, 1981; summarized in Wells and others, 1985). Data passes fold test as $k/k = 2.8$ is a statistically significant difference at 95% confidence level. "Reference Pole" taken from Diehl et al. (1983) "Latitude Shift at Site" (positive toward reference pole), and "Rotation of Site" (positive clockwise at site) found using TECTOROT. Tyee Fore-Arc Basin data taken from Simpson (1977).

Table 4. Chemical Analyses of the Siletz River Volcanics

Site	0W034	0W041	0W047	0W011	2W039	2W046	2W052	2W066	2W067
wt. %, volatile free									
SiO ₂	47.837	46.981	47.179	46.361	47.752	46.603	47.15	46.12	45.728
Al ₂ O ₃	13.737	14.181	13.679	14.261	14.252	15.003	14.45	14.22	14.128
Fe ₂ O ₃	13.437	13.481	13.479	13.261	12.352	12.503	12.25	13.82	14.028
MgO	6.717	6.911	7.089	7.151	7.432	7.633	7.64	7.44	7.478
CaO	11.937	11.881	11.579	11.861	12.352	12.303	12.65	10.82	10.928
Na ₂ O	2.697	2.711	3.209	2.991	2.452	2.403	2.48	2.89	3.108
K ₂ O	0.507	0.611	0.579	0.671	0.482	0.533	0.51	0.65	0.618
TiO ₂	2.097	2.131	2.079	2.161	1.892	1.873	1.86	2.8	2.728
P ₂ O ₅	0.507	0.531	0.539	0.621	0.492	0.533	0.48	0.65	0.648
MnO	0.527	0.581	0.589	0.661	0.542	0.613	0.53	0.59	0.608
Total	100	100	100	100	100	100	100	100	100
Na ₂ O + K ₂ O	3.204	3.322	3.788	3.662	2.934	2.936	2.99	3.54	3.726



The solid line represents a dividing line between alkalic and sub-alkalic magma series, taken from Miyashiro (1978)